Cellular/Molecular

Control of Sugar and Amino Acid Feeding via Pharyngeal Taste Neurons

Yu-Chieh David Chen,[1] Vaibhav Menon,[1] Ryan Matthew Joseph,[2] and Anupama Arun Dahanukar[1,2]
[1]Interdepartmental Neuroscience Program, University of California, Riverside, Riverside, California 92521, and [2]Department of Molecular, Cell, and Systems Biology, University of California, Riverside, Riverside, California 92521

Insect gustatory systems comprise multiple taste organs for detecting chemicals that signal palatable or noxious quality. Although much is known about how taste neurons sense various chemicals, many questions remain about how individual taste neurons in each taste organ control feeding. Here, we use the *Drosophila* pharynx as a model to investigate how taste information is encoded at the cellular level to regulate consumption of sugars and amino acids. We first generate taste-blind animals and establish a critical role for pharyngeal input in food selection. We then investigate feeding behavior of both male and female flies in which only selected classes of pharyngeal neurons are restored via binary choice feeding preference assays as well as Fly Liquid-Food Interaction Counter assays. We find instances of integration as well as redundancy in how pharyngeal neurons control behavioral responses to sugars and amino acids. Additionally, we find that pharyngeal neurons drive sugar feeding preference based on sweet taste but not on nutritional value. Finally, we demonstrate functional specialization of pharyngeal and external neurons using optogenetic activation. Overall, our genetic taste neuron protection system in a taste-blind background provides a powerful approach to elucidate principles of pharyngeal taste coding and demonstrates functional overlap and subdivision among taste neurons.

Key words: Drosophila; feeding; gustatory; pharynx; taste

Significance Statement

Dietary intake of nutritious chemicals such as sugars and amino acids is essential for the survival of an animal. In insects, distinct classes of taste neurons control acceptance or rejection of food sources. Here, we develop a genetic system to investigate how individual taste neurons in the *Drosophila* pharynx encode specific tastants, focusing on sugars and amino acids. By examining flies in which only a single class of taste neurons is active, we find evidence for functional overlap as well as redundancy in responses to sugars and amino acids. We also uncover a functional subdivision between pharyngeal and external neurons in driving feeding responses. Overall, we find that different pharyngeal neurons act together to control intake of the two categories of appetitive tastants.

Introduction

Taste sensilla, the functional taste sensory units in *Drosophila*, are distributed across the labellum, pharynx, legs, wing margins, and ovipositor. A typical taste sensillum contains two to four gustatory receptor neurons (GRNs), characterized by their responses to different categories of tastants such as sugars or bitter compounds. Over the past decade, the expression and function of several chemosensory receptors have been characterized in external taste neurons (Liman et al., 2014; Freeman and Dahanukar, 2015; Chen and Dahanukar, 2020). Systematic electrophysiological analyses of stimulus-evoked responses of labellar and tarsal sensilla have been conducted using panels of food tastants (Weiss et al., 2011; Ling et al., 2014) and have revealed the organization of GRNs that detect sweet and bitter tastants in various sensilla. Complementary transgenic reporter expression analyses of *Gr* and *Ir* genes have shown corresponding molecularly distinct classes of sensilla (Weiss et al., 2011; Koh et al., 2014; Ling et al., 2014; Fujii et al., 2015; Chen and Dahanukar, 2017).

Received July 12, 2020; revised May 6, 2021; accepted May 11, 2021.

Author contributions: Y.-C.D.C. and A.D. designed research; Y.-C.D.C., V.M., and R.M.J. performed research; Y.-C.D.C., V.M., and R.M.J. analyzed data; and Y.-C.D.C. and A.A.D. wrote the paper.

This work was supported by the Whitehall Foundation (Grant 2010-12-42), National Institutes of Health (Grants R01DC013587 and R01DC017390), and the University of California, Riverside Agricultural Experimental Station and National Institute of Food and Agriculture–U.S. Department of Agriculture (Hatch Project Grant 1011543). Y.-C.C. was a Howard Hughes Medical Institute International Student Research Fellow. We thank members of Dahanukar Lab for comments on the manuscript, Barbara Jablonska for generating the *Ir67c-LexA* line, John Carlson for the gift of the *Ir60b-LexA* line, and Nirao Shah and Hubert Amrein for sharing fly strains. Stocks were also obtained from the Bloomington Drosophila Stock Center (National Institutes of Health P40OD018537).

Y.-C.D. Chen's present address: New York University, New York, New York 10003.

R.M. Joseph's present address: Riverside City College, Riverside, CA 92506.

The authors declare no competing financial interests.

Correspondence should be addressed to Anupama Dahanukar at anupama.dahanukar@ucr.edu.

https://doi.org/10.1523/JNEUROSCI.1794-20.2021

An important step toward understanding principles of taste processing is to determine how responses elicited by distinct functional classes of GRNs are translated into different feeding behaviors. Functional roles of GRNs have largely been inferred from genetic silencing experiments (Chen and Dahanukar, 2020). However, assessment of the contribution of individual GRN classes is complicated by mounting evidence that some tastants can act on more than one class of GRNs (Weiss et al., 2011; Charlu et al., 2013; Ahn et al., 2017; Chen and Amrein, 2017; Joseph et al., 2017; Tauber et al., 2017; Jaeger et al., 2018; Devineni et al., 2019; Dweck and Carlson, 2020) and also that some GRNs sense more than one category of tastants (Charlu et al., 2013; Chen and Amrein, 2017; Ganguly et al., 2017; Jaeger et al., 2018; Chen et al., 2019). To address this question, we developed a genetic system to create flies in which only a single class of pharyngeal GRNs is active so that its role can be measured in the absence of all other taste input. Previous work has demonstrated roles for broad populations of *Gr64f* and *Ir76b* GRNs in driving feeding responses to sugars and amino acids, respectively (Dahanukar et al., 2007; Fujii et al., 2015; Ganguly et al., 2017). Recently, we described a map of molecular organization of pharyngeal GRNs (Chen and Dahanukar, 2017) and found evidence for combinatorial function of pharyngeal GRNs in driving behavioral responses to aversive substances (Chen et al., 2019). Here, we investigate how individual pharyngeal GRNs drive appetitive behavioral responses to sugars and amino acids.

We first generate taste-blind flies in which both internal and external GRNs are functionally absent, using *Ir25a-GAL4*, which we previously reported to be expressed in all pharyngeal GRNs, to drive expression of Kir2.1 in a *Pox-neuro* (*Poxn*) mutant background, in which external taste bristles are transformed into mechanosensory bristles (Nottebohm et al., 1992; Awasaki and Kimura, 1997; Chen et al., 2018). We report that appropriate feeding responses to both appetitive and aversive tastants are abolished in *Ir25a*-silenced *Poxn* taste-blind flies in binary choice assays, demonstrating a critical role for taste input in guiding short-term food choice decisions. Functional protection of selected pharyngeal GRNs in the taste-blind background shows that pharyngeal *Gr43a* GRNs promote feeding not only of sugar but also of amino acids. High-resolution quantitative analysis of feeding parameters reiterates the pharyngeal *Gr43a* GRN contribution to detection of sugars and amino acids. Genetic silencing experiments identify additional pharyngeal *Ir20a* GRNs that act with *Gr43a* GRNs to drive amino acid consumption, providing evidence for both functional overlap and redundancies in pharyngeal coding of appetitive tastants. On the other hand, distinctions between pharyngeal GRNs and external GRNs in feeding control are substantiated by optogenetic experiments, which show that activation of external sweet GRNs causes proboscis extension, whereas that of pharyngeal *Gr43a* GRNs does not. Together, our results identify coordinated action of distinct pharyngeal GRNs in controlling detection of appetitive tastants.

Materials and Methods

Fly strains. Flies were reared on standard cornmeal-dextrose-agar food at 25°C and 60–70% relative humidity under a 12 h/12 h dark/light cycle. The following fly lines were used: *Gr-GAL4* (Weiss et al., 2011; Ling et al., 2014), *Ir-GAL4* (Koh et al., 2014), *Ir76b-GAL4* (stock #41730, Bloomington Drosophila Stock Center), *Ir25a-GAL4* (stock #41728, Bloomington Drosophila Stock Center), *Ir100a-GAL4* (stock #41743, Bloomington Drosophila Stock Center), *ppk28-GAL4* (Cameron et al., 2010), *Gr43a-LexA* (Miyamoto and Amrein, 2014), *Gr32a-LexA* (Fan et al., 2013), *UAS-Kir2.1* (Baines et al., 2001), $Poxn^{\Delta M22\text{-}B5}$ (Boll and Noll, 2002), $Poxn^{70}$ (Awasaki and Kimura, 1997), *UAS-mCD8GFP* (Weiss et al., 2011), *UAS-CsChrimson* (stock #55136, Bloomington Drosophila Stock Center), *lexAop2-GAL80* (stock #32214, Bloomington Drosophila Stock Center), and *lexAop2-6XmCherry-HA* (stock #52271 and 52272, Bloomington Drosophila Stock Center). For experiments using *Poxn* mutants, we confirmed the *Poxn* mutant background in all sorted flies by observing the transformed long and bent mechanosensory hairs in the labellum, as well as the fused three tarsal segments in the legs. To generate the *Ir60b-LexA* line, both the 5′ and 3′ flanking regions of the Ir60b gene were used, as described previously (Koh et al., 2014). Assembled LexA vector was used to generate *Drosophila* strains through PhiC31 integration into attP2 landing sites (BestGene). To generate the *Ir67c-LexA* line, both the 5′ and 3′ flanking regions of the Ir67c gene were used, as described previously (Koh et al., 2014). Assembled LexA vector was used to generate *Drosophila* strains through a standard P-element transformation (BestGene).

Chemicals. Tastants obtained from Sigma are as follows: D-sucrose (catalog #S7903), glycerol (catalog #G9012), D-fructose (catalog #F0127), D-glucose (catalog #G6152), L-glucose (catalog #G5500), D-sorbitol (catalog #85529), D-mannose (catalog #M6020), D-arabinose (catalog #A3131), L-serine (catalog #84959), L-threonine (catalog #89179), L-phenylalanine (catalog #P5482), denatonium benzoate (caalog #D5765), and L-tartaric acid (catalog #251380). Sodium chloride was obtained from Macron Chemical (catalog #7581–06). All tastants were dissolved in water.

Immunohistochemistry. Flies were anesthetized on ice, and the proboscis and brain tissues were dissected in 1 × PBS with 0.3% Triton X-100 (PBST) and fixed for 30 min with 4% paraformaldehyde in 1 × PBST at room temperature. After three washes with 1 × PBST, samples were blocked with 5% normal goat serum (catalog #G9023, Sigma) in 1 × PBST. Tissues were incubated in primary antibody solutions for 3 d at 4°C. Primary antibodies were the following: mouse anti-nc82 (1:20; Developmental Studies Hybridoma Bank; RRID:AB_2314866), chicken anti-GFP (green fluorescent protein, 1:5000; catalog #ab13970, Abcam; RRID:AB_300798), and rabbit anti-DsRed (1:200; catalog #632496, Clontech; RRID:AB_10013483). Secondary antibodies (1:400; Invitrogen) were goat anti-chicken Alexa Fluor 488, goat anti-rabbit Alexa Fluor 546, and goat anti-mouse Alexa Fluor 647. Samples were mounted in VECTASHIELD Antifade Mounting Medium (catalog #H-1000, Vector Laboratories; RRID:AB_2336789) and stored at 4°C. Fluorescent images were acquired using a Leica SP5 confocal microscope with 400 Hz scan speed in 512 × 512 or 1024 × 1024 pixel formats. Image stacks were acquired at 1 μm optical sections. All images were presented as maximum projections of the *z* stack generated using Leica LAS AF software (Leica Microsystems).

Binary choice feeding assays. Feeding preference assays were performed as described previously (Charlu et al., 2013; Chen and Dahanukar, 2017). Briefly, flies 5–8 d old (10 males and 10 females) were starved for 24 h on water-saturated tissues and then placed in 50 mm × 9 mm tight-fit Petri dishes (catalog #35–1006, Falcon) with 18 10 μl dots of 0.75% agarose that alternated in tastant and color using either 0.25 mg/ml indigo carmine (catalog #I8130, Sigma) or 0.5 mg/ml sulforhodamine B (catalog #230162, Sigma). For all experiments, we swapped dyes for each tastant with similar numbers of trials to account for any dye preference. We noted that taste-blind flies (i.e., *Ir25a>Kir2.1 Poxn* flies) showed noticeable dye preferences for sulforhodamine B over indigo carmine. Although dye swap experiments annul the dye preference, the datasets reflect a high degree of variation in taste-blind flies. However, the observed dye bias is minimal when testing flies that have functional taste (e.g., *GAL4* and *UAS* control flies). Flies were allowed to feed for 2 h at 25°C in the dark, and the abdomen color was scored by dissecting the guts within 24 h. Trials with participation lower than 50% were excluded. Preference index (PI) was calculated as ((# of flies labeled with the tastant color) − (# of flies labeled with the control color))/(total number of flies that fed). In all cases, PI values were calculated for mixed populations of males and females, except for experiments with amino acids in which we used only females because they exhibit a stronger feeding preference for amino acids as compared with males.

Optogenetic activation. Experiments with *UAS-CsChrimson* were performed as described previously (Joseph et al., 2017), with the

following modifications. Flies were reared on standard cornmeal-dextrose-agar food at 25°C and 60–70% relative humidity under a 12 h/12 h dark/light cycle. Four days after eclosion, flies were transferred to standard cornmeal-dextrose-agar food supplemented with 1 mM all-trans-retinal (catalog #R2500, Sigma) and placed in the dark at 25°C for 3 d. Before testing, flies were briefly anesthetized with low amounts of CO_2 and were gently aspirated into 1000-µL pipette tips so that their heads protruded through the opening of the tip. Flies were placed under a standard dissecting microscope under low-light conditions and filmed with a 5.0-megapixel eyepiece digital camera with an exposure time of 500 ms (Model MD500, AmScope). Red light was provided at an intensity of ~5 mW/mm^2 by 626 nm LEDs (Super Bright LEDs). The testing protocol (see Fig. 8*A*) was as follows: flies were filmed in dark conditions for 15 s, after which red light was applied continuously for 15 s. Flies were then subjected to dark conditions for another 15 s, followed by another continuous application of red light for 15 s. Responses were classified as a full extension only if flies completely extended their proboscis, including the rostrum (see Fig. 8*C*). The order of genotypes tested on each day was randomized and tested blind to researchers. All the responses were scored blind to researchers to eliminate bias. Approximately equal numbers of males and females were tested.

Fly Liquid-Food Interaction Counter assay. The Fly Liquid-Food Interaction Counter (FLIC) *Drosophila* feeding behavior system (Sable Systems International) was used for measuring single-fly feeding behaviors. Feeding activities from three Drosophila Feeding Monitor (DFM) plates were collected by FLIC Monitor software version 2.1, which was described previously (Ro et al., 2014). Mated female flies aged 5–8 d were starved for 24 h in water-saturated vials before the assay. Flies were gently aspirated into individual arenas containing one of the tastants. The positions of tested genotypes and tastants on each DFM plate were randomly shuffled. Flies were assayed for 1 h, and features of the first feeding event were analyzed to avoid potential postingestive effects. A baseline electrical signal was calculated for each well by identifying the most commonly occurring electrical signal value throughout the assay period. Feeding events were defined as samples with an electrical signal over 100 arbitrary units (a.u.) plus baseline; tasting events were defined as samples with electrical signal over the baseline but <100 a.u. plus baseline. Two consecutive events were distinguished if they occurred >1 s apart. Analysis of FLIC raw data was conducted using custom R scripts. The first script analyzed the raw electrical signal data of each well to generate feeding features described throughout this article. A second script annotated each trial with its corresponding genotype and tastant information by extracting information from accompanying text files using character matching/extracting functions. A third script performed a logistic regression analysis using a model trained on a set of 400 randomly selected and manually sorted usable and unusable observations from our larger dataset of more than 3000 individual trials. Source codes and detailed descriptions of the feature extraction and model used in analysis can be obtained at https://github.com/vdmenon/FLIC.

Experimental design and statistical analyses. To analyze the behavioral differences between transgene controls and experimental groups (planned comparisons), we first checked the distribution of the data with a Kolmogorov–Smirnov test for normality. If the data were not normally distributed, a Kruskall–Wallis test, followed by the uncorrected Dunn's test, was used. If data were normally distributed, we used parametric one-way ANOVA followed by the uncorrected Fisher's least significant difference (LSD) test. In addition, a one sample *t* test (for normally distributed data) or Wilcoxon signed rank test (for not normally distributed data) was used to determine whether the preference indices were significantly different from zero, which represents no preference for either tastant in the binary choice feeding assays. For optogenetic experimental data (see Fig. 8), we used two-way ANOVA followed by Tukey's multiple comparisons test. All the experiments were performed in parallel with both control and experimental genotypes. The sample size for each experiment was based on previously published reports. All independent trials were performed over 2 d or more

Data availability. All original raw data in the article are available from Mendeley Data (doi: 10.17632/gg3v3sstgs.2).

Results

Flies lacking functional taste neurons fail to distinguish tastants in feeding choice assays

We recently described detailed receptor-to-neuron maps for the three pharyngeal taste organs in which we found that *Ir25a-GAL4* labels all 24 GRNs in the adult pharynx (Chen and Dahanukar, 2017). Taking advantage of the *Poxn* mutant (Nottebohm et al., 1992; Awasaki and Kimura, 1997), we created flies that lack all functional GRNs in external sensory bristles of the labellum, tarsi, and wing, and in the internal labral sense organs (LSO), ventral cibarial sense organs (VCSO), and dorsal cibarial sense organs (DCSO) by expressing the inwardly rectifying potassium channel *Kir2.1* via *Ir25a-GAL4* (Fig. 1*A–C*). We tested *Ir25a*-silenced *Poxn* flies, which are predicted to be true taste-blind flies, in a series of binary choice feeding assays to determine whether they were capable of making appropriate food choices in terms of appetitive responses to sugars and amino acids and aversive responses to bitter compounds or high concentrations of acid and salt when present in mixtures with sucrose.

We first offered flies a choice between two different concentrations of a sweet tastant—sucrose, glucose, fructose, or glycerol—and tested their feeding preference in binary choice assays. As expected, *GAL4* and *UAS* controls, which possess functional GRNs in the pharynx, showed robust preference for higher concentrations of each of these tastants over their counterparts at lower concentrations. Notably, *Ir25a*-silenced *Poxn* flies failed to distinguish between the different concentrations of sucrose (Fig. 1*D*), glucose (Fig. 1*E*), fructose (Fig. 1*F*), and glycerol (Fig. 1*G*; sucrose: $F_{(2,27)} = 11.97$, $p < 0.0001$ vs *UAS* control, $p = 0.0015$ vs *GAL4* control; glucose: $F_{(2,33)} = 3.994$, $p = 0.0164$ vs *UAS* control, $p = 0.0317$ vs *GAL4* control; fructose: $F_{(2,31)} = 6.256$, $p = 0.0033$ vs *UAS* control, $p = 0.0049$ vs *GAL4* control; glycerol: $F_{(2,31)} = 6.034$, $p = 0.0091$ vs *UAS* control, $p = 0.0047$ vs *GAL4* control; ANOVA; uncorrected Fisher's LSD test). We next tested amino acids, which are also appetitive stimuli. We performed preference assays with choices between 5 mM and 25 mM of individual amino acids (serine, threonine, or phenylalanine), which we previously reported to evoke appetitive feeding responses (Ganguly et al., 2017). Two of the amino acids, when tested individually, evoked mild preference for the higher concentration in both *GAL4* and *UAS* control flies (PI was significantly different from zero for *GAL4*, one sample *t* test, $p = 0.0368$ for serine, $p = 0.0363$ for threonine, $p = 0.4862$ for phenylalanine; and *UAS*, one sample *t* test, $p = 0.045$ for serine, $p = 0.0147$ for threonine, $p = 0.5410$ for phenylalanine). Although there were no significant differences between preference index values of control and *Ir25a*-silenced *Poxn* flies (Fig. 1*H–J*; serine: $F_{(2,27)} = 0.3254$, $p = 0.9292$ vs *UAS* control, $p = 0.5125$ vs *GAL4* control; threonine: $F_{(2,29)} = 1.683$, $p = 0.2181$ vs *UAS* control, $p = 0.0829$ vs *GAL4* control; phenylalanine: $F_{(2,27)} = 0.2553$, $p = 0.6029$ vs *UAS* control, $p = 0.5012$ vs *GAL4* control; ANOVA; uncorrected Fisher's LSD test), we found that preference indices of *Ir25a*-silenced *Poxn* flies were not significantly different from zero (one sample *t* test, $p = 0.2513$ for serine; $p = 0.7131$ for threonine; $p = 0.9136$ for phenylalanine). These results are consistent with the idea that the mild feeding response to serine and threonine is abolished in *Ir25a*-silenced *Poxn* flies. Because feeding preferences for individual amino acids were not very robust in this assay, we opted

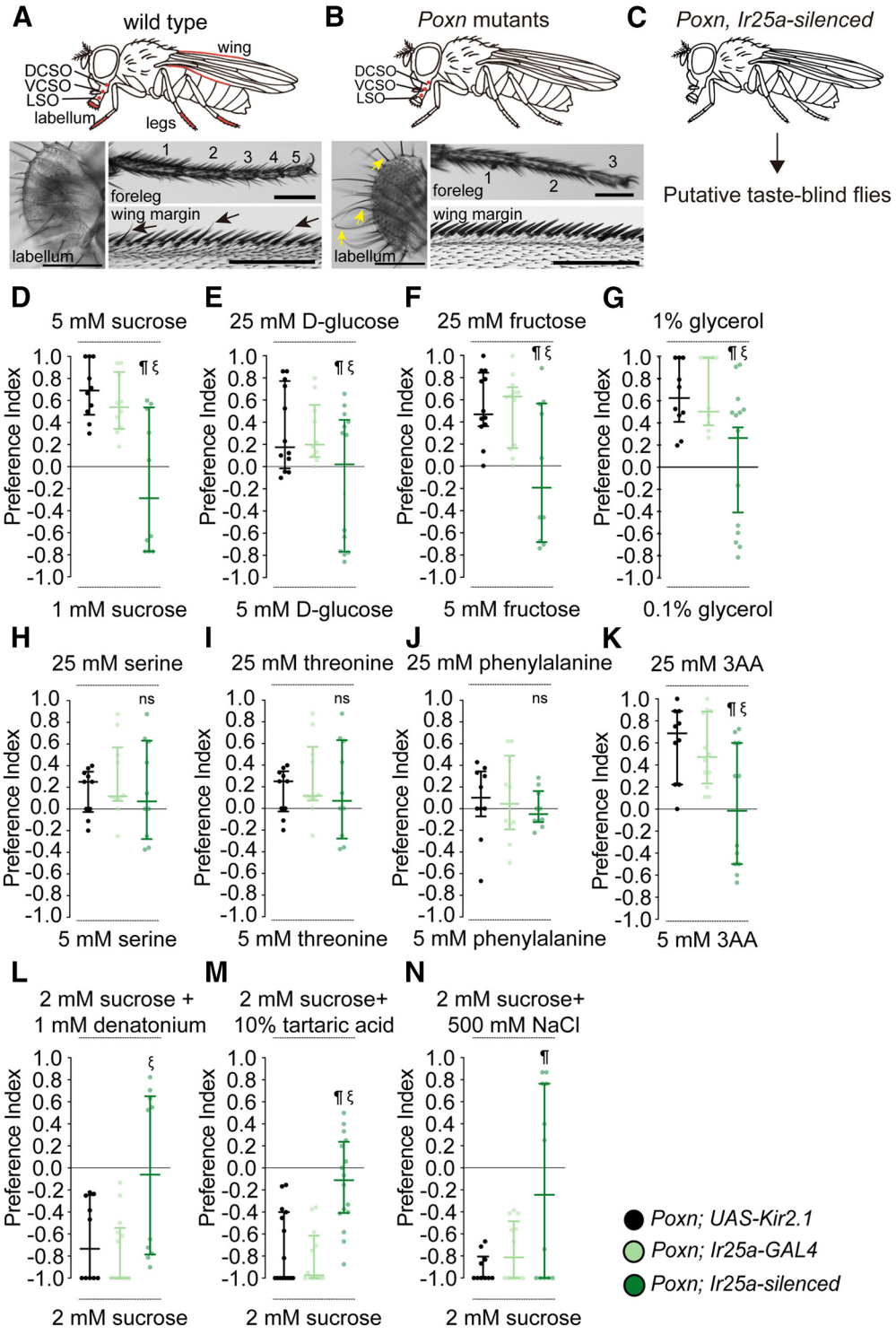

Figure 1. *Ir25a*-silenced *Poxn* flies are taste blind to tastants from different taste modalities. ***A–B***, Schematics (top) and bright field images of taste organs (bottom) in wild-type (***A***) and *Poxn* mutant (***B***) flies. The body parts marked in red indicate locations of taste neurons. Black arrows indicate taste hairs in the wing margins of wild-type animals, which are absent in *Poxn* mutants. Yellow arrows in the bright field image of the *Poxn* labellum point to representative long, bent mechanosensory bristles, which are present in place of external taste hairs. The five tarsal segments in wild-type forelegs are indicated by numbers; these are fused into three segments in *Poxn* mutants. Scale bar, 100 μm. ***C***, Schematic diagram showing the generation of taste-blind flies by silencing all pharyngeal neurons via *Ir25a-GAL4* in a *Poxn* mutant background. ***D–N***, Median preference index values of *Poxn* ($Poxn^{\Delta M22\text{-}B5}/Poxn^{70}$) mutants carrying indicated transgenes obtained from binary choice experiments with indicated tastants; 3AA is a mixture of serine, threonine, and phenylalanine. *UAS-Kir2.1* and *Ir25a-GAL4* transgenes were tested independently as indicated, or together (*Ir25a*-silenced); $n = 10–15$. Error bars indicate interquartile range; ¶ and ξ indicate a statistically significant difference from the *UAS* and *GAL4* controls, respectively, by one-way ANOVA followed by uncorrected Fisher's LSD test or Kruskal–Wallis test followed by uncorrected Dunn's test. The one sample *t* test or Wilcoxon signed rank test was used for testing whether the median values for each genotype were different from zero. ***D–N***, Genotypes, left to right, $Poxn^{\Delta M22\text{-}B5}/Poxn^{70}$; *UAS-Kir2.1/+* and $Poxn^{\Delta M22\text{-}B5}$, *Ir25a-GAL4*/$Poxn^{70}$; *Dr or TM3/+* and $Poxn^{\Delta M22\text{-}B5}$, *Ir25a-GAL4*/$Poxn^{70}$; *UAS-Kir2.1/UAS-Kir2.1*.

to test a mixture of the three amino acids. Given a choice between two concentrations of the same mixture, we found that control flies displayed a strong preference for a higher concentration of the three amino acid (3AA) mixture, which was lost in *Ir25a*-silenced *Poxn* flies (Fig. 1*K*; amino acids: $F_{(2,31)} = 6.207$, $p = 0.0035$ vs *UAS* control, $p = 0.0072$ vs *GAL4* control; ANOVA; uncorrected Fisher's LSD test). These results suggest that pharyngeal taste input is critical for discriminating the palatability of different concentrations of sweet and amino acid tastants.

We next tested whether *Ir25a*-silenced *Poxn* flies exhibited feeding avoidance of bitter (denatonium), acid (tartaric acid), and high salt (500 mM NaCl). In a previous study we found that *Ir25a*-silenced *Poxn* flies did not exert any preference when tested with 5 mM sucrose mixed with 1 mM denatonium or lobeline against 1 mM sucrose (Chen et al., 2019). In this study, we used a slightly modified feeding choice assay, in which all tastants were tested in a background concentration of sucrose (2 mM), which was used to stimulate feeding (Fig. 1*L–N*). Control flies showed robust avoidance of 1 mM denatonium, 10% tartaric acid, and 500 mM NaCl mixed with 2 mM sucrose, instead choosing 2 mM sucrose alone. Avoidance of all three tastants was completely abolished in *Ir25a*-silenced *Poxn* flies (in each case, the feeding preference index was not significantly different from zero; Wilcoxon signed rank test or one sample *t* test; $p = 0.4922$ for denatonium; $p = 0.2135$ for tartaric acid; $p = 0.2881$ for NaCl; Fig. 1*L–N*), consistent with our previous findings that pharyngeal taste input is critical for discriminating sugar/bitter mixtures from sugar alone (Chen et al., 2019). Together, these results suggest that pharyngeal GRNs detect both appetitive and aversive tastants and are capable of driving food choice in the absence of external taste input from the labellum and tarsi. Furthermore, any postingestive mechanisms, such as those described recently (Dus et al., 2011; Miyamoto et al., 2012; Stafford et al., 2012; Dus et al., 2015), do not appear to be sufficient to promote selection of appetitive tastants or avoidance of aversive tastants in short-term binary choice feeding assays when taste input is completely absent.

Pharyngeal *Gr43a* GRNs drive feeding choice of sucrose and amino acids

The *Ir25a*-silenced *Poxn* flies offered a genetic taste-blind background to investigate how individual neuron types encode tastants. Specifically, we determined which food choice parameters could be restored by functionally protecting defined classes of taste neurons in otherwise taste-blind flies. Flies in which pharyngeal GRNs labeled by a selected *chemoreceptor-LexA* driver were the only functional GRNs were created by expression of *lexAop2-GAL80* in an *Ir25a*-silenced *Poxn* background. In addition to the *chemoreceptor-LexA* drivers labeling sweet and bitter GRNs, *Gr43a-LexA* and *Gr32a-LexA*, respectively (Fan et al., 2013; Miyamoto and Amrein, 2014), we generated two additional *chemoreceptor-LexA* drivers that label single pharyngeal GRNs in the LSO (*Ir60b-LexA* and *Ir67c-LexA*). Consistent with previous expression results (Chen and Dahanukar, 2017), we validated expression of *Ir60b-LexA* and *Ir67c-LexA* drivers by examining colabeling of *Ir60b-LexA* and *Ir94f-GAL4* in the L7-7 neuron (Fig. 2*A*) and of *Ir67c-LexA* and *Ir67c-GAL4* in the L7-6 neuron (Fig. 2*B*).

To verify that the *chemoreceptor-LexA* > *lexAop2-GAL80* strategy would indeed suppress *GAL4*-dependent transgene expression in pharyngeal GRNs, we examined VCSO expression of *UAS-GFP* and *lexAop2-mCherry* in flies carrying *Ir76b-GAL4*, *Gr43a-LexA*, and *lexAop2-GAL80* transgenes. As we described previously (Chen and Dahanukar, 2017), *Ir76b-GAL4* labeled three neurons (V1-V3) in the VCSO, including two (V1 and V2) that are also labeled by *Gr43a-LexA* (Fig. 2*C*). In the presence of *lexAop2-GAL80*, we found GFP expression in V3 but not in the V1 and V2 neurons, confirming that *GAL4* activity was successfully restricted to pharyngeal *Gr43a* GRNs (Fig. 2*C*). We further validated this strategy for all four *chemoreceptor-LexA* > *lexAop2-GAL80* lines in flies carrying *Ir25a-GAL4* and *UAS-GFP* transgenes. As expected, in all cases, GFP expression was blocked in mCherry-expressing pharyngeal neurons (Fig. 2*D*).

We then crossed the four *chemosensory-LexA* drivers into the *Ir25a*-silenced *Poxn* taste-blind background to prevent expression of *UAS-Kir2.1* and protect selected GRNs from being silenced (*GrX/IrX*-protected *Poxn*). We tested *GrX/IrX*-protected *Poxn* flies for behavioral sensitivity to sucrose and the 3AA mixture in binary choice assays (Fig. 2*E–F*). As pharyngeal *Gr43a* GRNs are required for robust sugar consumption in *Poxn* mutants (LeDue et al., 2015), we first asked whether they were sufficient to drive selection of a higher, more appetitive, concentration of sucrose. As predicted, *Gr43a*-protected *Poxn* flies exhibited a strong preference for 5 mM sucrose over 1 mM sucrose (Fig. 2*E*; $p = 0.4007$ vs *UAS* control, $p = 0.9861$ vs *lexAop2-GAL80* control; Kruskal–Wallis test; uncorrected Dunn's test), showing that pharyngeal sugar-sensing *Gr43a* GRNs are sufficient to restore intensity discrimination and ingestion of sucrose. Unexpectedly, we found that feeding preference for a higher concentration of the 3AA mixture was also indistinguishable between *Gr43a*-protected *Poxn* flies and transgenic controls (Fig. 2*F*; $p = 0.422$ vs *UAS* control, $p = 0.6428$ vs *lexAop2-GAL80* control; Kruskal–Wallis test; uncorrected Dunn's test). Complementary experiments with similarly engineered flies carrying only one of the other three pharyngeal GRN types (*Gr32a*, *Ir60b*, and *Ir67c* GRNs) showed complete abolishment of behavioral responses to both sucrose and 3AA (in all cases, the feeding preference index was not significantly different from zero, Wilcoxon signed rank test or one sample *t* test; sucrose: $p = 0.9729$ for *Gr32a*-protected, $p = 0.7132$ for *Ir60b*-protected, $p = 0.8998$ for *Ir67c*-protected; 3AA: $p = 0.5625$ for *Gr32a*-protected, $p = 0.5899$ for *Ir60b*-protected, $p = 0.9677$ for *Ir67c*-protected; Fig. 2*E–F*). These results posit that pharyngeal *Gr43a* GRNs have the capacity to sense not only sugars but also amino acids.

Pharyngeal *Gr43a* GRNs alone partially restore feeding parameters for sugars and amino acids

GRNs in the pharyngeal canal are in an optimal location to regulate food intake. However, it is not clear whether, and if so how, individual features of feeding events are controlled by pharyngeal GRNs. To investigate this, we evaluated high-resolution feeding parameters in response to water, sugars, and amino acids in *UAS-Kir2.1 Poxn* control flies in which all pharyngeal GRNs are present and compared them with taste-blind flies (*Ir25a*-silenced *Poxn*; Figs. 3, 4). Feeding responses to different tastants were recorded using the FLIC (Ro et al., 2014; Fig. 3*A*). As described previously (Ro et al., 2014), tasting and feeding events were classified based on differences in output signal intensity, and we set a feeding threshold at 100 a.u. above baseline to separate the two. To exclude potential postingestive effects, we focused on peak intensity and duration of the first feeding event. All feeding responses with tastants were normalized to those obtained with water solvent alone. For sucrose, peak intensity and duration of

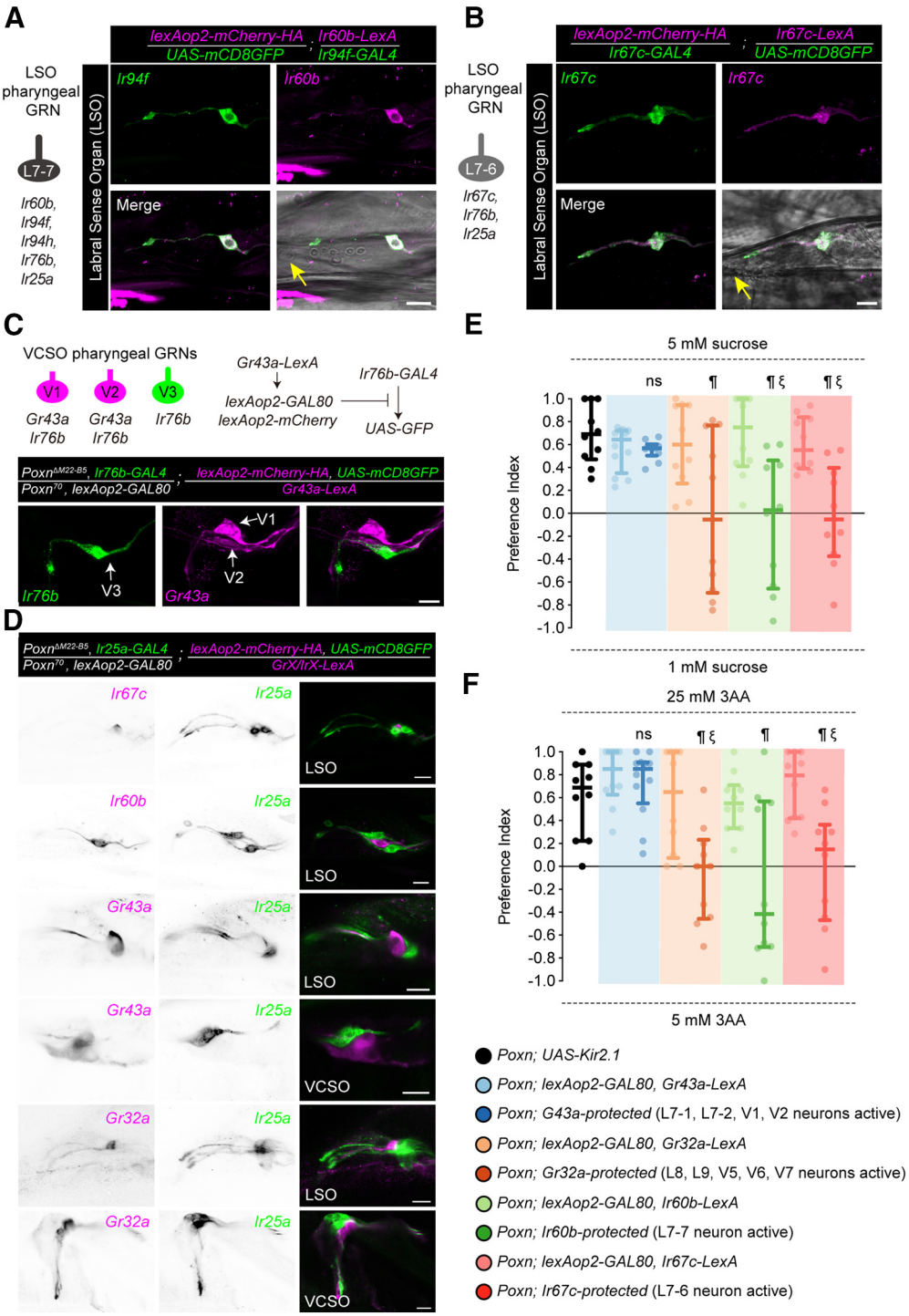

Figure 2. Feeding preferences of sugar and amino acids are recovered by functional restoration of pharyngeal *Gr43a* GRNs in taste-blind flies. ***A–B***, Validation of *Ir60b-LexA* and *Ir67c-LexA* in the LSO. Expression of *Ir94f-GAL4* (green) and *Ir60b-LexA* (magenta) or *I67c-GAL4* (green) and *Ir67c-LexA* (magenta) lines in the LSO is tested with *UAS-mCD8-GFP* and *lexAop2-mCherry-HA*. The colocalization of both reporters is observed in L7-7 neuron (***A***) and L7-6 neuron (***B***). The yellow arrows mark the #7 chemosensory sensillum of the LSO. Scale bar, 10 μm. Genotype (***A***), *lexAop2-mCherry-HA/UAS-mCD8-GFP; Ir60b-LexA/Ir94f-GAL4*, and (***B***) *lexAop2-mCherry-HA/Ir67c-GAL4; Ir67c-LexA/UAS-mCD8-GFP*. ***C***, Top left, Schematic diagram showing the transgenic reporter expression of *Gr43a* and *Ir76b* in three pharyngeal GRNs of the VCSO. Top right, Schematic diagram of genetic subtraction of *Gr43a-LexA* expression from *Ir76b-GAL4* with *lexAop2-GAL80*, which restricts *UAS-GFP* expression to nonoverlapping GRNs in the VCSO. Bottom, Colabeling of *Ir76b-GAL4*-driven *UAS-GFP* expression in the V3 neuron and *Gr43a-LexA*-driven *lexAop2-mCherry* (magenta) in the V1 and V2 neurons. Note that the GFP expression in V1 and V2 neurons is limited by the *lexAop2-GAL80* expression driven by *Gr43a-LexA*. Scale bar, 10 μm. Genotype, *Poxn$^{\Delta M22\text{-}B5}$, Ir76b-GAL4/Poxn^{70}, lexAop2-GAL80; lexAop2-mCherry-HA, UAS-mCD8-GFP/Gr43a-LexA*. ***D***, Colabeling of *Ir25a-GAL4*-driven *UAS-GFP* expression and indicated *Chemoreceptor-LexA*-driven *lexAop2-mCherry* (magenta) in LSO and/or VCSO neurons. Scale bar, 10 μm. Genotype, *Poxn$^{\Delta M22\text{-}B5}$, Ir25a-GAL4/Poxn^{70}, lexAop2-GAL80; lexAop2-mCherry-HA, UAS-mCD8-GFP/(Gr43a, or Gr32a or Ir60b or Ir67c)-LexA*. ***E–F***, Median preference index values of *Poxn* (*Poxn$^{\Delta M22\text{-}B5}$/Poxn^{70}*) mutants carrying indicated transgenes obtained from binary choice experiments with 5 mM sucrose tested against 1 mM sucrose (***E***) or 25 mM 3AA mixtures tested against 5 mM 3AA (***F***). The *lexAop2-GAL80* with *Gr43a-LexA*, *Gr32a-LexA*, *Ir60b-LexA*, and *Ir67c-LexA* transgene controls were tested independently as indicated, or together with *Gr43a*-protected, *Gr32a*-protected, *Ir60b*-protected, and *Ir67c*-protected in a taste-blind background (*Poxn, Ir25a*-silenced). The *UAS-Kir2.1* transgene control data were the same as shown in Figure 1*D*,*K*; $n = 10–15$. Error bars indicate interquartile range; ¶ and ξ indicate a statistically significant difference from the *UAS* and *GAL4* controls, respectively, by Kruskal–Wallis test followed by uncorrected Dunn's test. The Wilcoxon signed rank test was used for testing whether the median values

the first feeding event were significantly reduced in taste-blind flies as compared with control flies (Fig. 3*B*; Mann–Whitney test, peak intensity, $p < 0.0001$; peak duration, $p < 0.0001$). Thus, lack of taste input has an impact on feeding parameters in a manner that weakens consumption of sugars.

To investigate which subsets of pharyngeal GRNs control peak intensity and duration of the first feeding event, we measured these parameters in flies that possess only single classes of pharyngeal GRNs. For this purpose, we genetically protected selected classes of GRNs in *Ir25a*-silenced *Poxn* flies (Fig. 3*C*). We chose GRNs that are known or predicted to be appetitive (*Gr43a*), deterrent (*Gr32a*), modulatory (*Ir60b*), or of unknown (*Ir67c*) function. As compared with the *Ir25a*-silenced *Poxn* flies, we found that functional restoration of *Gr43a* GRNs caused consistent increases in both intensity and duration of the first feeding event in response to sucrose (Fig. 3*C*; peak intensity: Kruskal–Wallis statistics = 24.89, *Gr43a*-protected vs *Ir25a*-silenced, $p = 0.0059$; peak duration: Kruskal—Wallis statistics = 47.69, *Gr43a*-protected vs *Ir25a*-silenced, $p < 0.0001$). By contrast, these parameters were not affected, or were slightly reduced, in flies in which either *Gr32a*, *Ir60b*, or *Ir67c* pharyngeal GRNs were protected (Fig. 3*C*; peak intensity: Kruskal–Wallis statistics = 24.89, *Gr32a*-protected vs *Ir25a*-silenced, $p = 0.0148$). We also evaluated how *Gr43a*-protection influenced first feeding event parameters for two other sweet tastants, fructose and glycerol (Fig. 3*D–E*). For both compounds, protection of *Gr43a* neurons restored the peak intensity and duration of the first feeding event, although to varying extents (fructose peak intensity: Kruskal–Wallis statistics = 39.19, *UAS* control vs *Ir25a*-silenced, $p < 0.0001$; *Gr43a*-protected vs *Ir25a*-silenced, $p < 0.0001$; *UAS* control vs *Gr43a*-protected, $p = 0.1696$; fructose peak duration: Kruskal–Wallis statistics = 75.08, *UAS* control vs *Ir25a*-silenced, $p < 0.0001$; *Gr43a*-protected vs *Ir25a*-silenced, $p < 0.0001$; *UAS* control vs *Gr43a*-protected, $p = 0.003$; glycerol peak intensity: Kruskal–Wallis statistics = 12.29, *UAS* control vs *Ir25a*-silenced, $p = 0.0019$; *Gr43a*-protected vs *Ir25a*-silenced, $p = 0.0022$; *UAS* control vs *Gr43a*-protected, $p = 0.9725$; glycerol peak duration: Kruskal–Wallis statistics = 64.07, *UAS* control vs *Ir25a*-silenced, $p < 0.0001$; *Gr43a*-protected vs *Ir25a*-silenced, $p < 0.0001$; *UAS* control vs *Gr43a*-protected, $p = 0.3398$). These results support the idea that pharyngeal *Gr43a* GRNs control parameters of feeding events in response to various sweet tastants.

Because pharyngeal *Gr43a* neurons drove preference for a 3AA mixture in choice assays (Fig. 2*F*), we next evaluated parameters of the first feeding event of this mixture. Similar to the results obtained with sweet tastants, we found that the peak intensity and duration of the first feeding event were significantly reduced in taste-blind flies as compared with control flies (Fig. 4*A*; Mann–Whitney test, peak intensity, $p < 0.0001$; peak duration, $p < 0.0001$). Protection of *Gr43a* GRNs significantly increased the intensity and duration of the first feeding event in response to 3AA as compared with that observed in *Ir25a*-silenced *Poxn* flies (Fig. 4*B*; peak intensity: Kruskal–Wallis statistics = 30.45, *Gr43a*-protected vs *Ir25a*-silenced, $p < 0.0001$; peak duration: Kruskal–Wallis statistics = 25.65, *Gr43a*-protected vs *Ir25a*-silenced, $p < 0.0001$). Interestingly, protection of either *Ir60b* or *Ir67c* GRNs also caused a slight increase in duration of the first 3AA feeding event (Fig. 4*B*; peak duration: Kruskal–Wallis statistics = 25.65, *Ir60b*-protected vs *Ir25a*-silenced, $p = 0.0057$; *Ir67c*-protected vs *Ir25a*-silenced, $p = 0.0067$). Together, these results suggest that pharyngeal *Gr43a* input plays a role in controlling amino acid intake. Moreover, *Ir60b* and/or *Ir67c* neurons may also contribute to 3AA detection, which was not uncovered in binary choice assays (Fig. 2*F*).

We observed that the 3AA mixture evokes an increase in peak intensity as well as in duration of the first feeding event. One possibility is that different components of the 3AA mixture have differential effects on these parameters. We thus tested the three amino acids individually (serine, threonine, phenylalanine) using taste-blind and *Gr43a*-protected *Poxn* flies (Fig. 4*C–E*). As predicted, the duration of the first feeding event was depressed in taste-blind flies as compared with *UAS* controls, although the changes in peak intensity observed in taste-blind flies were surprising (no change for serine, increase in peak intensity for threonine and phenylalanine). In all three instances, protection of *Gr43a* neurons had no effect on the peak intensity (serine peak intensity: Kruskal–Wallis statistics = 2.81, *UAS* control vs *Ir25a*-silenced, $p = 0.451$; *Gr43a*-protected vs *Ir25a*-silenced, $p = 0.0996$; *UAS* control vs *Gr43a*-protected, $p = 0.3276$; threonine peak intensity: Kruskal–Wallis statistics = 9.77, *UAS* control vs *Ir25a*-silenced, $p = 0.0442$; *Gr43a*-protected vs *Ir25a*-silenced, $p = 0.3965$; *UAS* control vs *Gr43a*-protected, $p = 0.002$; phenylalanine peak intensity: Kruskal–Wallis statistics = 9.326, *UAS* control vs *Ir25a*-silenced, $p = 0.0027$; *Gr43a*-protected vs *Ir25a*-silenced, $p = 0.2594$; *UAS* control vs *Gr43a*-protected, $p = 0.0553$), but at least partially restored feeding duration (serine peak duration: Kruskal–Wallis statistics = 62.31, *UAS* control vs *Ir25a*-silenced, $p < 0.0001$; *Gr43a*-protected vs *Ir25a*-silenced, $p < 0.0001$; *UAS* control vs *Gr43a*-protected, $p = 0.0093$; threonine peak duration: Kruskal–Wallis statistics = 53.03, *UAS* control vs *Ir25a*-silenced, $p < 0.0001$; *Gr43a*-protected vs *Ir25a*-silenced, $p < 0.0001$; *UAS* control vs *Gr43a*-protected, $p = 0.0039$; phenylalanine peak duration: Kruskal–Wallis statistics = 65.65, *UAS* control vs *Ir25a*-silenced, $p < 0.0001$; *Gr43a*-protected vs *Ir25a*-silenced, $p < 0.0001$; *UAS* control vs *Gr43a*-protected, $p = 0.0003$). Altogether, these results lend support to the notion that pharyngeal *Gr43a* GRNs promote feeding of individual amino acids mainly by sustaining feeding duration. Moreover, although individual amino acids did not affect feeding intensity, mixtures of amino acids may act synergistically to do so.

Functional redundancies in pharyngeal GRNs for sensing amino acids

As pharyngeal *Gr43a* GRNs sense both sugars and amino acids, an expectation is that silencing of these neurons will disrupt behavioral responses to sugars as well as amino acids. As reported previously (LeDue et al., 2015), genetic inactivation of pharyngeal GRNs in *Poxn* flies via *Gr64e-GAL4,* which labels the same pharyngeal *Gr43a* GRNs (Chen and Dahanukar, 2017), abolished feeding preference for the higher concentration of sucrose and fructose, indicating that these neurons are necessary for intensity discrimination of sugar (Fig. 5*A–B*; sucrose: $F_{(2,31)} = 22.29$, $p < 0.0001$ vs *UAS* control, $p = 0.0001$ vs *GAL4* control; fructose: $F_{(2,31)} = 3.037$, $p = 0.037$ vs *UAS* control, $p = 0.0391$ vs *GAL4* control; ANOVA; uncorrected Fisher's LSD test). However, in

←

for each genotype were different from zero. Genotypes, left to right, $Poxn^{\Delta M22\text{-}B5}/Poxn^{70}$; *UAS-Kir2.1/+* and $Poxn^{\Delta M22\text{-}B5}/Poxn^{70}$, *lexAop2-GAL80*; *Gr43a-LexA/+* and $Poxn^{\Delta M22\text{-}B5}$, *Ir25a-GAL4/*$Poxn^{70}$, *lexAop2-GAL80*; *Gr43a-LexA/UAS-Kir2.1* and $Poxn^{\Delta M22\text{-}B5}/Poxn^{70}$, *lexAop2-GAL80*; *Gr32a-LexA/+* and $Poxn^{\Delta M22\text{-}B5}$, *Ir25a-GAL4/*$Poxn^{70}$, *lexAop2-GAL80*; *Gr32a-LexA/UAS-Kir2.1* and $Poxn^{\Delta M22\text{-}B5}/Poxn^{70}$, *lexAop2-GAL80*; *Ir60b-LexA/+* and $Poxn^{\Delta M22\text{-}B5}$, *Ir25a-GAL4/*$Poxn^{70}$, *lexAop2-GAL80*; *Ir60b-LexA/UAS-Kir2.1* and $Poxn^{\Delta M22\text{-}B5}/Poxn^{70}$, *lexAop2-GAL80*; *Ir67c-LexA/+* and $Poxn^{\Delta M22\text{-}B5}$, *Ir25a-GAL4/*$Poxn^{70}$, *lexAop2-GAL80*; *Ir67c-LexA/UAS-Kir2.1*.

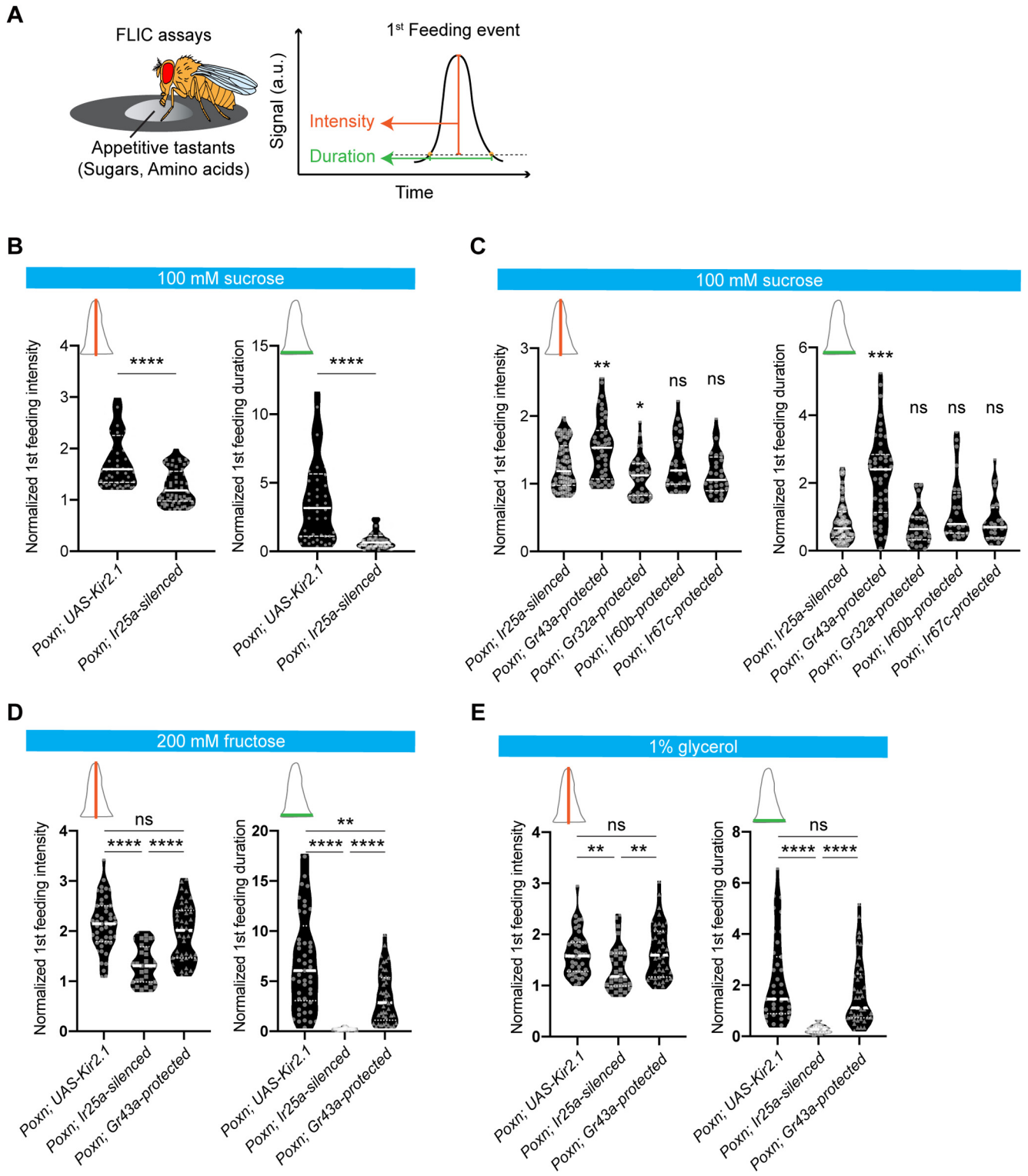

Figure 3. Pharyngeal GRNs regulate microfeeding features in response to sweet tastants. ***A***, Schematic diagram of FLIC setup (left). Feeding responses to water and appetitive tastants (sugars and amino acids) were tested. Schematic diagram showing distinct features of microfeeding behaviors extracted by our custom R scripts (right). ***B***, Feeding intensity and duration of the first feeding event in response to 100 mM sucrose was compared between *UAS* control (*Poxn; UAS-Kir2.1*) and taste blind (*Poxn; Ir25a*-silenced). All the features of microfeeding behaviors were normalized to their corresponding water values before comparison; $n = 57–77$. White horizontal solid and dashed lines indicate median and the first and third quartiles, respectively. Asterisks indicate significant difference between two groups by Mann–Whitney test; $^{****}p < 0.0001$. Genotypes, left to right, $Poxn^{\Delta M22\text{-}B5}/Poxn^{70}$; *UAS-Kir2.1/+* and $Poxn^{\Delta M22\text{-}B5}$, *Ir25a-GAL4/*$Poxn^{70}$; *UAS-Kir2.1/UAS-Kir2.1*. ***C***, Feeding intensity and duration of the first feeding event in response to 100 mM sucrose was compared between taste-blind (*Poxn; Ir25a*-silenced) and flies with restoring selected pharyngeal GRNs as indicated. All the features of microfeeding behaviors were normalized to their corresponding water values before comparison; $n = 25–74$. White horizontal solid and dashed lines indicate median and the first and third quartiles, respectively. Asterisks indicate significant difference from taste-blind (*Poxn; Ir25a*-silenced) flies by Kruskal–Wallis test followed by uncorrected Dunn's test; $^{*}p < 0.05$, $^{**}p < 0.01$, $^{***}p < 0.001$. ns, Not significant. Genotypes, left to right, $Poxn^{\Delta M22\text{-}B5}$, *Ir25a-GAL4/*$Poxn^{70}$; *UAS-Kir2.1/UAS-Kir2.1* and $Poxn^{\Delta M22\text{-}B5}$, *Ir25a-GAL4/*$Poxn^{70}$, *lexAop2-GAL80*; *Gr43a-LexA/UAS-Kir2.1* and $Poxn^{\Delta M22\text{-}B5}$, *Ir25a-GAL4/*$Poxn^{70}$, *lexAop2-GAL80*; *Gr32a-LexA/UAS-Kir2.1* and $Poxn^{\Delta M22\text{-}B5}$, *Ir25a-GAL4/*$Poxn^{70}$, *lexAop2-GAL80*; *Ir60b-LexA/UAS-Kir2.1* and $Poxn^{\Delta M22\text{-}B5}$, *Ir25a-GAL4/*$Poxn^{70}$, *lexAop2-GAL80*; *Ir67c-LexA/UAS-Kir2.1*. ***D–E***, Feeding intensity and duration of the first feeding event in response to

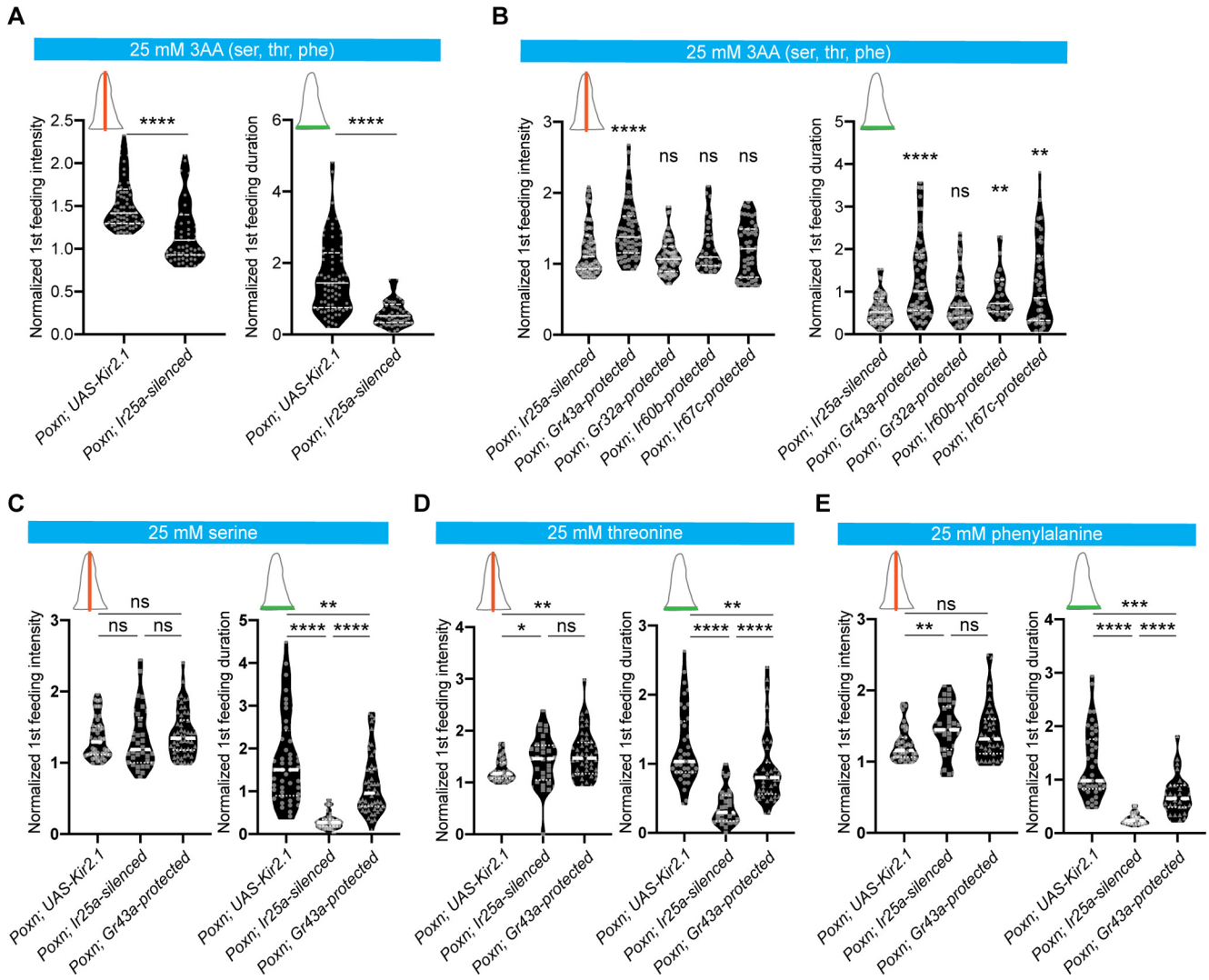

Figure 4. Pharyngeal GRNs regulate microfeeding features in response to amino acids. ***A***, Feeding intensity and duration of the first feeding event in response to 25 mM 3AA (ser, thr, phe) was compared between *UAS* control (*Poxn; UAS-Kir2.1*) and taste blind (*Poxn; Ir25a*-silenced). All the features of microfeeding behaviors were normalized to their corresponding water values before comparison; $n = 65–78$. White horizontal solid and dashed lines indicate median and the first and third quartiles, respectively. Asterisks indicate significant difference between two groups by Mann–Whitney test; $^{****}p < 0.0001$. Genotypes, left to right, $Poxn^{\Delta M22\text{-}B5}/Poxn^{70}$; *UAS-Kir2.1/+* and $Poxn^{\Delta M22\text{-}B5}$, *Ir25a-GAL4/*$Poxn^{70}$; *UAS-Kir2.1/UAS-Kir2.1*. ***B***, Feeding intensity and duration of the first feeding event in response to 25 mM 3AA (ser, thr, phe) was compared between taste blind (*Poxn; Ir25a*-silenced) and flies with restoring selected pharyngeal GRNs as indicated. All the features of microfeeding behaviors were normalized to their corresponding water values before comparison; $n = 25–71$. White horizontal solid and dashed lines indicate median and the first and third quartiles, respectively. Asterisks indicate significant difference from taste-blind (*Poxn; Ir25a*-silenced) flies by Kruskal–Wallis test followed by uncorrected Dunn's test; $^{**}p < 0.01$, $^{****}p < 0.0001$. ns, Not significant. Genotypes, left to right, $Poxn^{\Delta M22\text{-}B5}$, *Ir25a-GAL4/*$Poxn^{70}$; *UAS-Kir2.1/UAS-Kir2.1* and $Poxn^{\Delta M22\text{-}B5}$, *Ir25a-GAL4/*$Poxn^{70}$, *lexAop2-GAL80*; *Gr43a-LexA/UAS-Kir2.1* and $Poxn^{\Delta M22\text{-}B5}$, *Ir25a-GAL4/*$Poxn^{70}$, *lexAop2-GAL80*; *Gr32a-LexA/UAS-Kir2.1* and $Poxn^{\Delta M22\text{-}B5}$, *Ir25a-GAL4/*$Poxn^{70}$, *lexAop2-GAL80*; *Ir60b-LexA/UAS-Kir2.1* and $Poxn^{\Delta M22\text{-}B5}$, *Ir25a-GAL4/*$Poxn^{70}$, *lexAop2-GAL80*; *Ir67c-LexA/UAS-Kir2.1*. ***C–E***, Feeding intensity and duration of the first feeding event in response to 25 mM serine (***C***), 25 mM threonine (***D***), or 25 mM phenylalanine (***E***) was compared between *UAS* control (*Poxn; UAS-Kir2.1*), taste-blind (*Poxn; Ir25a*-silenced), and *Gr43a*-protected *Poxn* flies. All the features of microfeeding behaviors were normalized to their corresponding water values before comparison; $n = 28–56$. White horizontal solid and dashed lines indicate median and the first and third quartiles, respectively. Asterisks indicate significant difference from taste-blind (*Poxn; Ir25a*-silenced) flies by Kruskal–Wallis test followed by uncorrected Dunn's test; $^{*}p < 0.05$, $^{**}p < 0.01$, $^{***}p < 0.001$, $^{****}p < 0.0001$. ns, Not significant. Genotypes, left to right, $Poxn^{\Delta M22\text{-}B5}/Poxn^{70}$; *UAS-Kir2.1/+* and $Poxn^{\Delta M22\text{-}B5}$, *Ir25a-GAL4/*$Poxn^{70}$; *UAS-Kir2.1/UAS-Kir2.1* and $Poxn^{\Delta M22\text{-}B5}$, *Ir25a-GAL4/*$Poxn^{70}$, *lexAop2-GAL80*; *Gr43a-LexA/UAS-Kir2.1*.

←

200 mM fructose (***D***) or 1% glycerol (***E***) was compared between *UAS* control (*Poxn; UAS-Kir2.1*), taste-blind (*Poxn; Ir25a*-silenced), and *Gr43a*-protected *Poxn* flies. All the features of microfeeding behaviors were normalized to their corresponding water values before comparison; $n = 30–49$. White horizontal solid and dashed lines indicate median and the first and third quartiles, respectively. Asterisks indicate significant difference from taste-blind (*Poxn; Ir25a*-silenced) flies by Kruskal–Wallis test followed by uncorrected Dunn's test; $^{**}p < 0.01$, $^{****}p < 0.0001$. ns, Not significant. Genotypes, left to right, $Poxn^{\Delta M22\text{-}B5}/Poxn^{70}$; *UAS-Kir2.1/+* and $Poxn^{\Delta M22\text{-}B5}$, *Ir25a-GAL4/*$Poxn^{70}$; *UAS-Kir2.1/UAS-Kir2.1* and $Poxn^{\Delta M22\text{-}B5}$, *Ir25a-GAL4/*$Poxn^{70}$, *lexAop2-GAL80*; *Gr43a-LexA/UAS-Kir2.1*.

similar experiments with 3AA mixtures, feeding preference for the higher concentration was not significantly reduced in *Gr64e*-silenced *Poxn* flies (Fig. 5*C*; Kruskal–Wallis test, $p = 0.1134$ vs *UAS* control, $p = 0.3231$ vs *GAL4* control; uncorrected Dunn's test), arguing that other classes of pharyngeal GRNs may also be involved in sensing amino acids.

To identify these additional pharyngeal GRNs, we selected a tool kit based on our previous mapping results (Chen and Dahanukar, 2017) and manipulated different, and in some instances overlapping, subsets of pharyngeal GRNs, including the following: putative bitter GRNs labeled by *Gr66a-/Gr93d-*

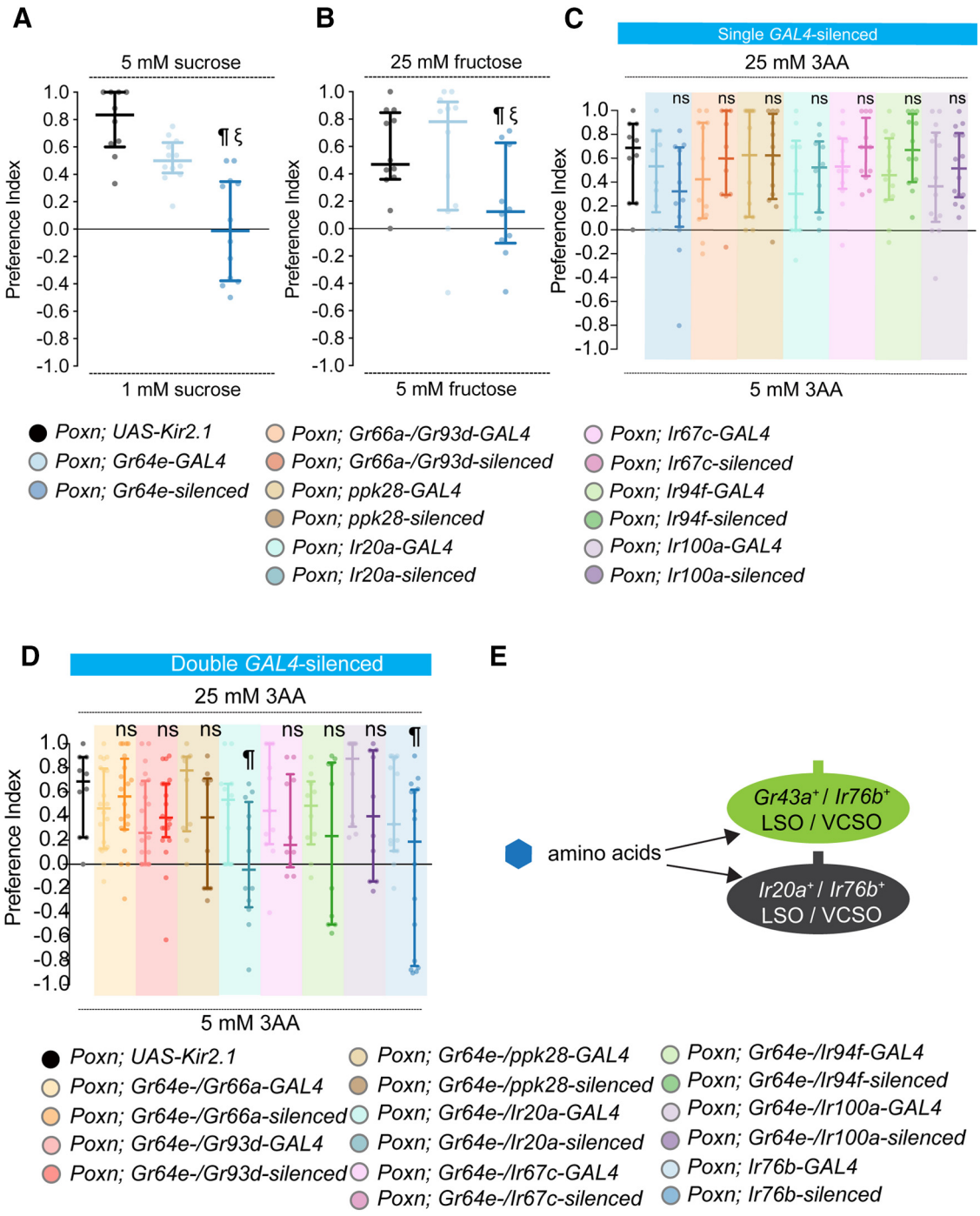

Figure 5. Pharyngeal *Gr43a* and *Ir20a* GRNs are necessary for feeding preference for amino acids. ***A–D***, Median preference index values of *Poxn* ($Poxn^{\Delta M22\text{-}B5}/Poxn^{70}$) mutants carrying indicated transgenes obtained from binary choice experiments with indicated sugars (***A***, ***B***) or a mixture of serine, threonine and phenylalanine (***C***, ***D***). *UAS-Kir2.1* and *Gr/Ir-GAL4* transgenes were tested independently as indicated or together (*Gr/Ir*-silenced). Note that the *UAS-Kir2.1* data were the same as those shown in Figure 1*D*,*K*; $n = 10–20$. Error bars indicate interquartile range; ¶ and ξ indicate a statistically significant difference from the *UAS* and *GAL4* controls, respectively, by Kruskal–Wallis test followed by uncorrected Dunn's test. ***A–D***, Genotypes, left to right, (***A***, ***B***) $Poxn^{\Delta M22\text{-}B5}/Poxn^{70}$; *UAS-Kir2.1/+* and $Poxn^{\Delta M22\text{-}B5}$, *Gr64e-GAL4/Poxn*^{70} and $Poxn^{\Delta M22\text{-}B5}$, *Gr64e-GAL4/Poxn*^{70}; *UAS-Kir2.1/+* (***C***) $Poxn^{\Delta M22\text{-}B5}/Poxn^{70}$; *UAS-Kir2.1/+* and $Poxn^{\Delta M22\text{-}B5}$, *Gr64e-GAL4/Poxn*^{70} and $Poxn^{\Delta M22\text{-}B5}$, *Gr64e-GAL4/Poxn*^{70}; *UAS-Kir2.1/+* and $Poxn^{\Delta M22\text{-}B5}$, *Gr66a-GAL4/Poxn*^{70}; *Gr93d-GAL4/+* and $Poxn^{\Delta M22\text{-}B5}$, *Gr66a-GAL4/Poxn*^{70}; *Gr93d-GAL4/UAS-Kir2.1* and $Poxn^{\Delta M22\text{-}B5}/Poxn^{70}$; *ppk28-GAL4/+* and $Poxn^{\Delta M22\text{-}B5}/Poxn^{70}$; *ppk28-GAL4/UAS-Kir2.1* and $Poxn^{\Delta M22\text{-}B5}$, *Ir20a-GAL4/Poxn*^{70}; *Dr or TM3/+* and $Poxn^{\Delta M22\text{-}B5}$, *Ir20a-GAL4/Poxn*^{70}; *UAS-Kir2.1/ Dr or TM3* and $Poxn^{\Delta M22\text{-}B5}$, *Ir67c-GAL4/Poxn*^{70}; *Dr or TM3/+* and $Poxn^{\Delta M22\text{-}B5}$, *Ir67c-GAL4/Poxn*^{70}; *UAS-Kir2.1/Dr or TM3* and $Poxn^{\Delta M22\text{-}B5}/Poxn^{70}$; *Ir94f-GAL4/+* and $Poxn^{\Delta M22\text{-}B5}/Poxn^{70}$; *Ir94f-GAL4/UAS-Kir2.1* and $Poxn^{\Delta M22\text{-}B5}/Poxn^{70}$; *Ir100a-GAL4/+* and $Poxn^{\Delta M22\text{-}B5}/Poxn^{70}$; *Ir100a-GAL4/UAS-Kir2.1* (***D***) $Poxn^{\Delta M22\text{-}B5}/Poxn^{70}$; *UAS-Kir2.1/+* and $Poxn^{\Delta M22\text{-}B5}$, *Gr64e-GAL4/Poxn*^{70}; *Gr66a-GAL4/+* and $Poxn^{\Delta M22\text{-}B5}$, *Gr64e-GAL4/Poxn*^{70}; *Gr66a-GAL4/UAS-Kir2.1* and $Poxn^{\Delta M22\text{-}B5}$, *Gr64e-GAL4/Poxn*^{70}; *Gr93d-GAL4/+* and $Poxn^{\Delta M22\text{-}B5}$, *Gr64e-GAL4/Poxn*^{70}; *Gr93d-GAL4/UAS-Kir2.1* and $Poxn^{\Delta M22\text{-}B5}$, *Gr64e-GAL4/Poxn*^{70}; *ppk28-GAL4/+* and $Poxn^{\Delta M22\text{-}B5}$, *Gr64e-GAL4/Poxn*^{70}; *ppk28-GAL4/UAS-Kir2.1* and $Poxn^{\Delta M22\text{-}B5}$, *Ir20a-GAL4/Poxn*^{70}; *Gr64e-GAL4/+* and $Poxn^{\Delta M22\text{-}B5}$, *Ir20a-GAL4/Poxn*^{70}; *Gr64e-GAL4/UAS-Kir2.1* and $Poxn^{\Delta M22\text{-}B5}$, *Ir67c-GAL4/Poxn*^{70}; *Gr64e-GAL4/+* and $Poxn^{\Delta M22\text{-}B5}$, *Ir67c-GAL4/Poxn*^{70}; *Gr64e-GAL4/UAS-Kir2.1* and $Poxn^{\Delta M22\text{-}B5}$, *Gr64e-GAL4/Poxn*^{70}; *Ir94f-GAL4/+* and $Poxn^{\Delta M22\text{-}B5}$, *Gr64e-GAL4/Poxn*^{70}; *Ir94f-GAL4/UAS-Kir2.1* and $Poxn^{\Delta M22\text{-}B5}$, *Gr64e-GAL4/Poxn*^{70}; *Ir100a-GAL4/+* and $Poxn^{\Delta M22\text{-}B5}$, *Gr64e-GAL4/Poxn*^{70}; *Ir100a-GAL4/UAS-Kir2.1* and $Poxn^{\Delta M22\text{-}B5}$, *Ir76b-GAL4/Poxn*^{70}; *Dr or TM3/+* and $Poxn^{\Delta M22\text{-}B5}$, *Ir76b-GAL4/Poxn*^{70}; *UAS-Kir2.1/UAS-Kir2.1*. ***E***, Schematic diagram showing detection of amino acids through two populations of pharyngeal GRNs.

GAL4 (L7-3, L8, L9, V5-V8), putative water GRNs labeled by *ppk28-GAL4* (L7-4, L7-5, V4), and other *Ir*-expressing GRNs labeled by *GAL4* drivers for *Ir20a* (L7-4, L7-5, V3, V4), *Ir67c* (L7-6), *Ir94f* (L7-7) and *Ir100a* (L7-8, DD3, DP3). We found that independently silencing any of these subsets of pharyngeal GRNs did not diminish behavioral sensitivity to the 3AA mixture (Fig. 5*C*; Kruskal–Wallis test; *Gr66a-/Gr93a*-silenced: $p = 0.9539$ vs *UAS* control, $p = 0.479$ vs *GAL4* control; *ppk28*-silenced: $p = 0.9836$ vs *UAS* control, $p = 0.9433$ vs *GAL4* control; *Ir20a*-silenced: $p = 0.4507$ vs *UAS* control, $p = 0.612$ vs *GAL4* control; *Ir67c*-silenced: $p = 0.6413$ vs *UAS* control, $p = 0.4108$ vs *GAL4* control; *Ir94f*-silenced: $p = 0.5553$ vs *UAS* control, $p = 0.1617$ vs *GAL4* control; *Ir100a*-silenced: $p = 0.6996$ vs *UAS* control, $p = 0.5411$ vs *GAL4* control; uncorrected Dunn's test). A possible explanation for this observation is that more than one class of amino acid–sensing pharyngeal GRNs act in redundant neural circuits to promote amino acid intake.

Given that our results establish a role for pharyngeal *Gr43a* GRNs in driving amino acid choice and consumption (Figs. 2*F*, 4*B*), we silenced pharyngeal GRNs in pairwise combinations with *Gr64e* GRNs and tested resulting double-silenced flies for loss of feeding response to amino acids. Notably, silencing of both *Gr64e* and *Ir20a* GRNs affected the flies' ability to discriminate between 5 mM and 25 mM 3AA mixtures as compared with *GAL4* controls (Fig. 5*D*; Kruskal–Wallis test; *Gr64e-/Ir20a*-silenced: $p = 0.0058$ vs *UAS* control, $p = 0.0538$ vs *GAL4* control; uncorrected Dunn's test). No other driver combinations had a similar effect (Kruskal–Wallis test; *Gr64e-/Gr66a*-silenced: $p = 0.7139$ vs *UAS* control, $p = 0.5637$ vs *GAL4* control; *Gr64e-/Gr93a*-silenced: $p = 0.265$ vs *UAS* control, $p = 0.6499$ vs *GAL4* control; *Gr64e-/ppk28*-silenced: $p = 0.1365$ vs *UAS* control, $p = 0.1061$ vs *GAL4* control; *Gr64e-/Ir67c*-silenced: $p = 0.1476$ vs *UAS* control, $p = 0.2819$ vs *GAL4* control; *Gr64e-/Ir94f*-silenced: $p = 0.1134$ vs *UAS* control, $p = 0.5583$ vs *GAL4* control; *Gr64e-/Ir100a*-silenced: $p = 0.4103$ vs *UAS* control, $p = 0.1153$ vs *GAL4* control; uncorrected Dunn's test). Behavioral sensitivity to amino acids was reduced in *Ir76b*-silenced *Poxn* flies (Kruskal–Wallis test; *Ir76b*-silenced: $p = 0.0143$ vs *UAS* control, $p = 0.0533$ vs *GAL4* control; uncorrected Dunn's test), which were generated with an *Ir76b-GAL4* driver that labels pharyngeal *Gr43a* GRNs as well as other *Ir* GRNs, including *Ir20a* GRNs. Together, our results suggest that appetitive amino acids are sensed by at least two different types of pharyngeal GRNs, *Gr43a* and *Ir20a* (Fig. 5*E*).

Pharyngeal *Gr43a* GRNs promote food choice based on sweet taste but not nutritional value of sugars

Food choice is immediately influenced by sweet taste and over time by caloric content of food (Stafford et al., 2012). Several nutrient sensors that play a part in the latter have been identified in the fly brain, including DH44 neurons in the pars intercerebralis (Dus et al., 2015) and *Gr43a* neurons in the posterior superior lateral protocerebrum (Miyamoto et al., 2012), both of which sense nutrient sugar levels in the hemolymph. Although peripheral sweet GRNs are known to detect chemicals perceived as sweet to humans (Dahanukar et al., 2007; Slone et al., 2007; Jiao et al., 2008; Fujii et al., 2015; LeDue et al., 2015), little is known about whether they can distinguish sugars based on nutritional value. We therefore wished to investigate the relative contribution of sweet taste and nutritive value in sugar feeding choice mediated by pharyngeal *Gr43a* GRNs. We first tested behavioral sensitivity to L-glucose, an enantiomer of the natural D-glucose with no caloric value (Fig. 6*A*), and D-glucose (Fig. 6*B*) in choice assays with 50 mM and 200 mM concentrations. Wild-type (w^{1118}), *UAS-Kir2.1 Poxn* controls, and *Gr43a*-protected *Poxn* flies all showed a strong preference for 200 mM L-glucose over 50 mM L-glucose (Wilcoxon signed rank test or one sample *t* test; $p = 0.002$ for w^{1118}, $p = 0.002$ for *UAS* control, $p < 0.0001$ for *Gr43a*-protected), consistent with previous reports of sweetness of L-glucose (Stafford et al., 2012). Taste-blind flies (*Ir25a*-silenced *Poxn* flies), as well as flies in which only one of the other three pharyngeal GRNs (*Gr32a*, *Ir60b*, and *Ir67c* GRNs) were protected, showed a loss of intensity discrimination, consistent with an inability to sense L-glucose (Fig. 6*A*; Wilcoxon signed rank test or one sample *t* test; $p = 0.9401$ for *Ir25a*-silenced, $p = 0.5566$ for *Gr32a*-protected, $p = 0.5039$ for *Ir60b*-protected, $p = 0.7251$ for *Ir67c*-protected). Similar results were observed in feeding choice assays with 50 mM and 200 mM of D-glucose (Fig. 6*B*; Wilcoxon signed rank test or one sample *t* test; $p < 0.0001$ for w^{1118}, $p = 0.0002$ for *UAS* control, $p = 0.9732$ for *Ir25a*-silenced, $p < 0.0001$ for *Gr43a*-protected, $p = 0.3667$ for *Gr32a*-protected, $p = 0.4294$ for *Ir60b*-protected, $p = 0.6426$ for *Ir67c*-protected). Thus, flies with pharyngeal *Gr43a* GRNs alone can carry out intensity discrimination of both L-glucose and D-glucose.

We next evaluated preference between D-glucose (nutritive) and L-glucose (non-nutritive) in feeding choice assays in which both tastants were presented at 50 mM. We found that w^{1118} flies, but not *UAS-Kir2.1 Poxn* control flies, showed a strong preference for 50 mM D-glucose over 50 mM L-glucose (Wilcoxon signed rank test or one sample *t* test; $p = 0.0039$ for w^{1118}, $p = 0.5616$ for *UAS* control), suggesting that the presence or absence of external taste neurons yields different behavioral sensitivities to D-glucose and L-glucose. Interestingly, among all genotypes tested in a *Poxn* mutant background, we found that *Gr43a*-protected *Poxn* flies exhibited a strong preference for 50 mM D-glucose over 50 mM L-glucose (Fig. 6*C*; Wilcoxon signed rank test or one sample *t* test; $p = 0.6869$ for *Ir25a*-silenced, $p < 0.0001$ for *Gr43a*-protected, $p = 0.2456$ for *Gr32a*-protected, $p = 0.3308$ for *Ir60b*-protected, $p = 0.6633$ for *Ir67c*-protected). Thus, the function of *Gr43a* GRNs, when no other GRNs are present, was able to recapitulate the behavioral preference observed in wild-type flies. Importantly, although *Gr43a* is expressed in a few nutrient-sensing neurons in the protocerebrum (Miyamoto et al., 2012) and enteroendocrine cells in the gut (Park and Kwon, 2011), these locations are not intersected by *Ir25a-GAL4* and *Gr43a-LexA* and are thus unlikely to account for the observed phenotypes. Specifically, *Ir25a-GAL4* did not label any cells in the gut. Also, examination of *Ir25a-GAL4* and *Gr43a-LexA* expression in the brain showed that *Ir25a-GAL4* did not label any neurons in the protocerebrum of flies either 7 or 14 d old (Extended Data Fig. 1-1). Thus, *Gr43a* neurons in the protocerebrum are expected to remain functional in all genotypes that were tested. In addition, *Gr43a-LexA*-labeled neurons in the protocerebrum were visible in older flies (14 d old) but not in younger flies (7 d old) that were used in behavioral assays (Extended Data Fig. 1-1). Thus, an intriguing alternative is that other pharyngeal GRNs can detect glucose and interfere with discrimination between D-glucose and L-glucose in *Poxn* flies.

In *Gr43a*-protected *Poxn* flies, we considered whether the *Gr43a* GRN circuits encode nutritional value and drive preference for nutritive tastants over non-nutritive ones. We therefore tested feeding preference for mixtures of various concentrations of D-sorbitol and D-mannose with 50 mM L-glucose, offered in binary choice assays with 50 mM D-glucose. Both D-sorbitol and D-mannose are nutritious but not sweet (Stafford et al., 2012).

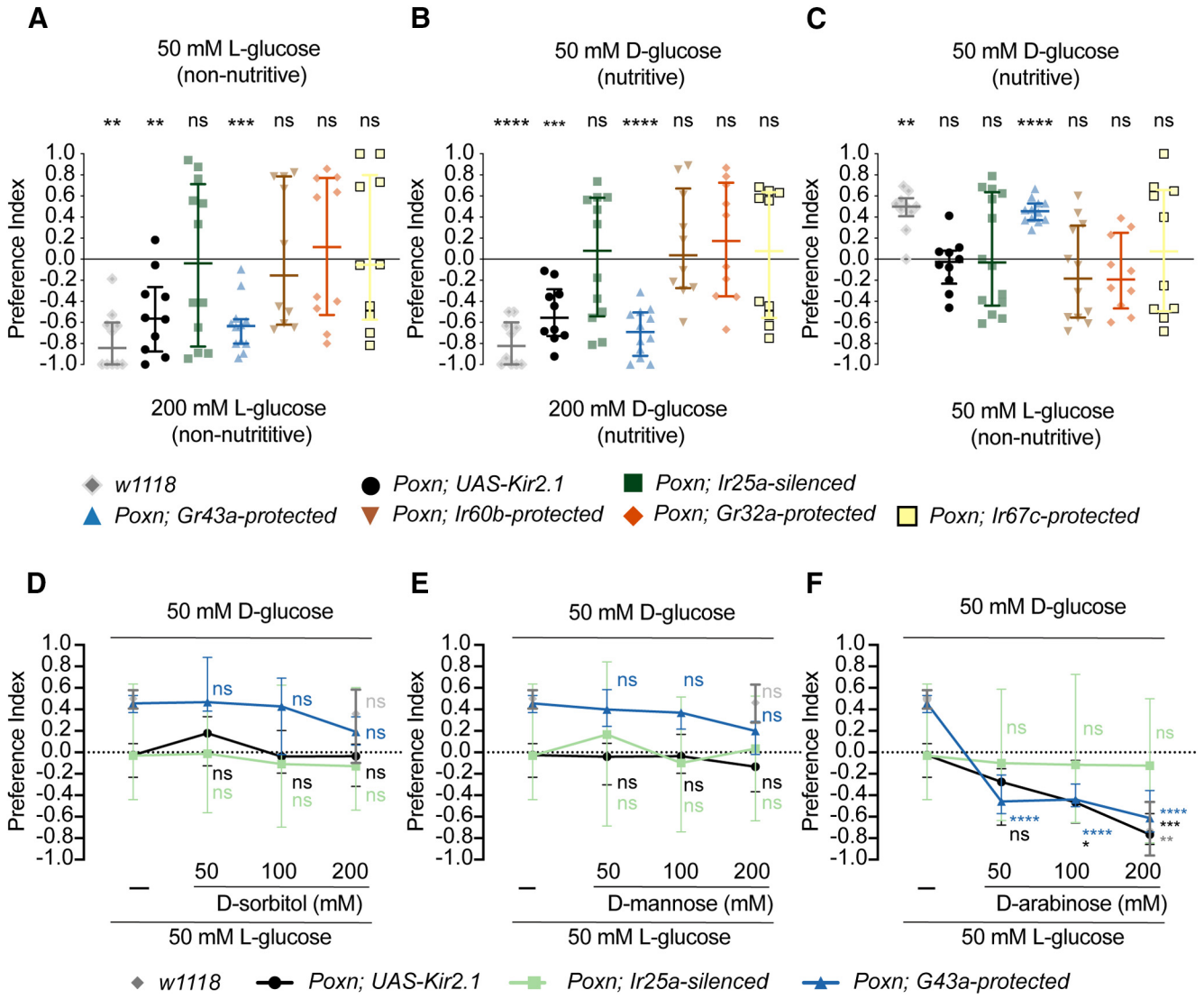

Figure 6. Pharyngeal *Gr43a* neurons promote food choice mainly based on sweet taste but not nutritional value of sugars. ***A–C***, Median preference index values of *Poxn* (*Poxn*$^{\Delta M22\text{-}B5}$/*Poxn*^{70}) mutants carrying indicated transgenes obtained from binary choice experiments with 50 mM L-glucose tested against 200 mM L-glucose (***A***), 50 mM D-glucose tested against 200 mM D-glucose (***B***), and 50 mM D-glucose tested against 50 mM L-glucose (***C***); $n = 10–14$. Error bars indicate interquartile range. The Wilcoxon signed rank test or one sample *t* test was used for testing whether the median values for each genotype were different from zero; $^{**}p < 0.01$, $^{***}p < 0.001$, $^{****}p < 0.0001$. ns, Not significant. Genotype, left to right, *w*^{1118}, *Poxn*$^{\Delta M22\text{-}B5}$/*Poxn*^{70}; *UAS-Kir2.1/+*, *Poxn*$^{\Delta M22\text{-}B5}$, *Ir25a-GAL4/Poxn*^{70}; *UAS-Kir2.1/UAS-Kir2.1* and *Poxn*$^{\Delta M22\text{-}B5}$, *Ir25a-GAL4/Poxn*^{70}, *lexAop2-GAL80*; *Gr43a-LexA/UAS-Kir2.1* and *Poxn*$^{\Delta M22\text{-}B5}$, *Ir25a-GAL4/Poxn*^{70}, *lexAop2-GAL80*; *Ir60b-LexA/UAS-Kir2.1* and *Poxn*$^{\Delta M22\text{-}B5}$, *Ir25a-GAL4/Poxn*^{70}, *lexAop2-GAL80*; *Gr32a-LexA/UAS-Kir2.1* and *Poxn*$^{\Delta M22\text{-}B5}$, *Ir25a-GAL4/Poxn*^{70}, *lexAop2-GAL80*; *Ir67c-LexA/UAS-Kir2.1*. ***D–F***, Median preference index values of *Poxn* (*Poxn*$^{\Delta M22\text{-}B5}$/*Poxn*^{70}) mutants carrying indicated transgenes obtained from binary choice experiments with 50 mM D-glucose tested against 50 mM L-glucose mixed with various concentrations of D-sorbitol (***D***), D-mannose (***E***), and D-arabinose (***F***); $n = 10–14$. Error bars indicate interquartile range. Asterisks indicate significant difference from 50 mM L-glucose alone within the same genotype by two-way ANOVA with *post hoc* uncorrected Fisher's LSD test; $^{*}p < 0.05$, $^{**}p < 0.01$, $^{***}p < 0.001$, $^{****}p < 0.0001$. ns, Not significant. Genotype from left to right, *w*^{1118} and *Poxn*$^{\Delta M22\text{-}B5}$/*Poxn*^{70}; *UAS-Kir2.1/+* and *Poxn*$^{\Delta M22\text{-}B5}$, *Ir25a-GAL4/Poxn*^{70}; *UAS-Kir2.1/UAS-Kir2.1* and *Poxn*$^{\Delta M22\text{-}B5}$, *Ir25a-GAL4/Poxn*^{70}, *lexAop2-GAL80*; *Gr43a-LexA/UAS-Kir2.1*.

Therefore, any increase in feeding preference for L-glucose mixtures with these compounds would indicate that *Gr43a*-protected *Poxn* flies can choose tastants based on caloric value rather than sweetness alone. However, we found that *Gr43a*-protected *Poxn* flies continued to exhibit a strong preference for 50 mM D-glucose over L-glucose/D-sorbitol and L-glucose/D-mannose mixtures at all concentrations tested (Fig. 6*D–E*). The *UAS-Kir2.1 Poxn* control flies also showed no further increase in feeding preference for L-glucose/D-sorbitol and L-glucose/D-mannose mixtures as compared with L-glucose alone (D-sorbitol: $F_{(2,114)} = 15.24$, $p = 0.4933$ *UAS* control 0 vs 50 mM D-sorbitol, $p = 0.8134$ *UAS* control 0 vs 100 mM D-sorbitol, $p = 0.6794$ *UAS* control 0 vs 200 mM D-sorbitol; D-mannose: $F_{(2,114)} = 12.35$, $p = 0.8928$ *UAS* control 0 vs 50 mM D-mannose, $p = 0.9466$ *UAS* control 0 vs 100 mM D-mannose, $p = 0.3812$ *UAS* control 0 vs 200 mM D-mannose; two-way ANOVA; uncorrected Fisher's LSD test). In contrast, when D-arabinose (sweet, non-nutritive; Stafford et al., 2012) was mixed with L-glucose, feeding preference of *UAS-Kir2.1 Poxn* control flies (D-arabinose: $F_{(2,114)} = 6.961$, $p = 0.0953$ *UAS* control 0 vs 50 mM D-arabinose, $p = 0.0471$ *UAS* control 0 vs 100 mM D-arabinose, $p = 0.0005$ *UAS* control 0 vs 200 mM D-arabinose; two-way ANOVA; uncorrected Fisher's LSD test) as well as *Gr43a*-protected *Poxn* flies shifted from 50 mM D-glucose to the L-glucose/D-arabinose mixtures at all concentrations tested (Fig. 6*F*; D-arabinose: $F_{(2,114)} = 6.961$, $p < 0.0001$ *Gr43a*-protected 0 vs 50 mM D-arabinose, $p < 0.0001$

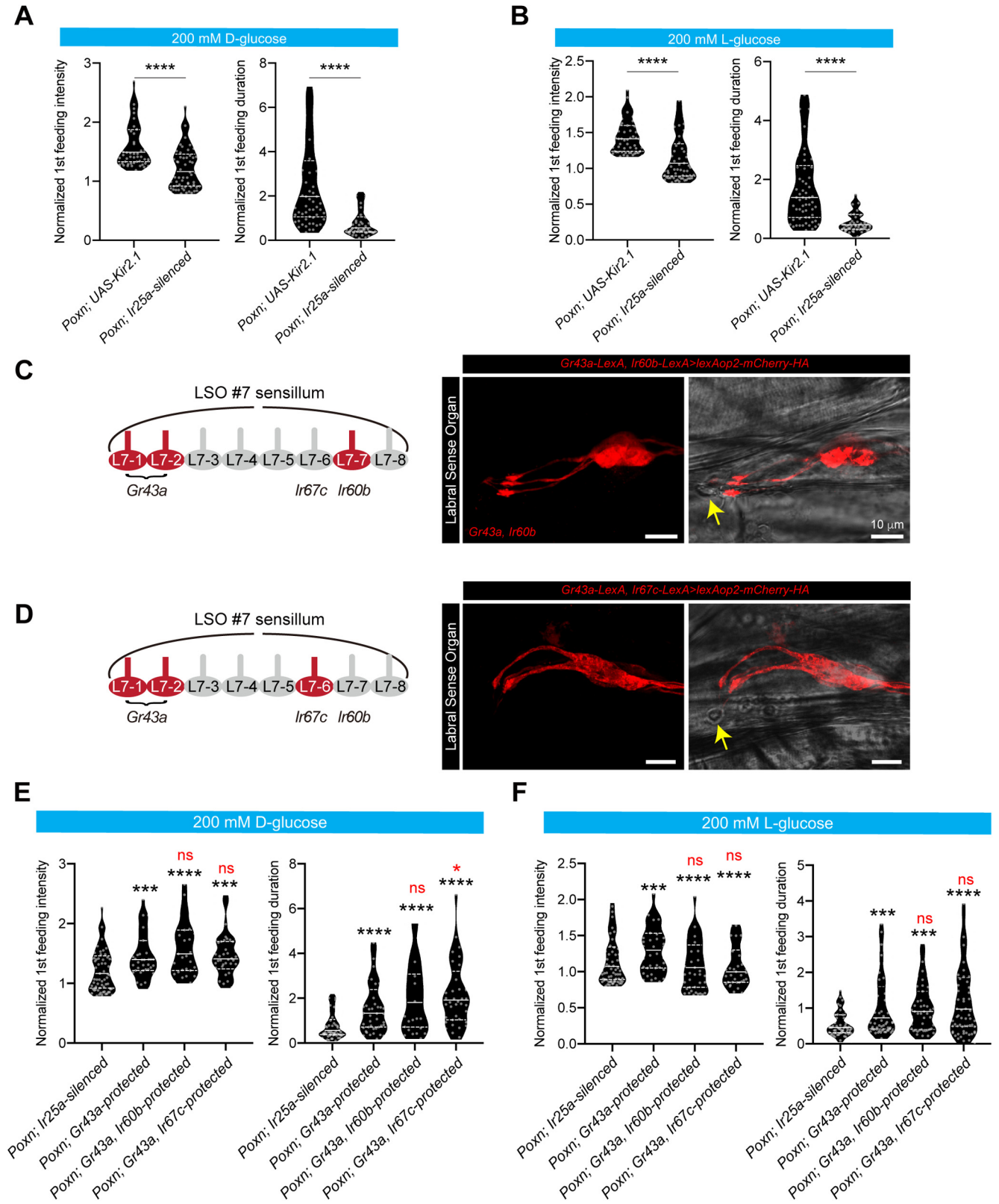

Figure 7. Pharyngeal *Gr43a* GRNs along with pharyngeal *Ir67c* GRNs differentially regulate micro-feeding responses to D-glucose but not L-glucose. ***A–B***, Feeding intensity and duration of the first feeding event in response to 200 mM D-glucose (***A***) and L-glucose (***B***) was compared between *UAS* control (*Poxn; UAS-Kir2.1*) and taste blind (*Poxn; Ir25a*-silenced). All the features of microfeeding behaviors were normalized to their corresponding water values before comparison; $n = 64–77$. White horizontal solid and dashed lines indicate median and the first and third quartiles, respectively. Asterisks indicate significant difference between two groups by Mann–Whitney test; ****$p < 0.0001$. Genotypes, left to right, $Poxn^{\Delta M22\text{-}B5}/Poxn^{70}$; *UAS-Kir2.1/+* and $Poxn^{\Delta M22\text{-}B5}$, *Ir25a-GAL4/*$Poxn^{70}$; *UAS-Kir2.1/UAS-Kir2.1*. ***C–D***, The mCherry reporter expressions (red) driven by recombinant transgenes containing *Gr43a-LexA/Ir60b-LexA* (***C***) and *Gr43a-LexA/Ir67c-LexA* (***D***) in the #7 sensillum of LSO. Yellow arrows indicate the cuticular pore of the #7 sensillum of LSO. Scale bar, 10 μm. ***E–F***, Feeding intensity and duration of the first feeding event in response to 200 mM D-glucose (***E***) or 200 mM L-glucose (***F***) was compared between taste-blind (*Poxn; Ir25a*-silenced), *Gr43a*-protected *Poxn* flies, *Gr43a/Ir60b*-protected *Poxn* flies, and *Gr43a/Ir67c*-protected *Poxn* flies. All the features of microfeeding behaviors were normalized to their corresponding water values before comparison; $n = 30–79$. White horizontal solid and

Gr43a-protected 0 vs 100 mM D-arabinose, $p < 0.0001$ *Gr43a*-protected 0 vs 200 mM D-arabinose; two-way ANOVA; uncorrected Fisher's LSD test). Similar phenotypes were observed for w^{1118} flies, which were tested with mixtures containing the highest concentration of D-sorbitol, D-mannose, or D-arabinose mixtures ($p = 0.5906$ for w^{1118} 0 vs 200 mM D-sorbitol; $p = 0.6971$ for w^{1118} 0 vs 200 mM D-mannose; $p < 0.0001$ for w^{1118} 0 vs 200 mM D-arabinose; Mann–Whitney test). Taste-blind flies remained neutral in all assays. Altogether, these results are consistent with the idea that pharyngeal *Gr43a* GRNs promote food choice based on sweet taste but not on the nutritional value of sugars.

Ir67c GRNs differently modulate *Gr43a* GRN-driven feeding responses to D-glucose

Our binary feeding preference results showed that pharyngeal *Gr43a* GRN alone can discriminate the intensity difference of both D-glucose and L-glucose (Fig. 6*A–B*), so we next tested how protection of pharyngeal *Gr43a* GRNs contribute to the feeding parameters to D-glucose and L-glucose in FLIC assays. We first found that the peak intensity and duration of the first feeding event to both D-glucose and L-glucose were significantly reduced in taste-blind flies as compared with control flies (Fig. 7*A–B*; D-glucose: Mann–Whitney test, peak intensity, $p < 0.0001$, peak duration, $p < 0.0001$; L-glucose: Mann–Whitney test, peak intensity, $p < 0.0001$, peak duration, $p < 0.0001$), suggesting that pharyngeal GRNs control these feeding parameters.

We next asked whether protection of *Gr43a* GRNs alone can restore the feeding parameters to both D-glucose and L-glucose. Because pharyngeal *Gr43a* GRNs are necessary for stimulating consumption of various sugars (Fig. 3*C–E*), we reasoned that any other GRN circuits that control sugar feeding would do so via some functional interaction with *Gr43a* GRN circuits. To test this, we generated otherwise taste-blind flies in which *Gr43a* GRNs were protected in combination with either *Ir60b* or *Ir67c* GRNs using *LexA* drivers. We chose *Ir60b* and *Ir67c* GRNs because they each label single pharyngeal GRNs in sensillum #7 of the LSO (Chen and Dahanukar, 2017). Recombinant chromosomes with combinations of *LexA* transgenes were validated by visualizing reporter expression in three pharyngeal GRNs of the LSO (Fig. 7*C–D*). We found that functional restoration of *Gr43a* GRNs caused consistent increases in both intensity and duration of the first feeding event in response to D-glucose (Fig. 7*E*; D-glucose peak intensity: Kruskal–Wallis statistics = 22.7, *Gr43a*-protected vs *Ir25a*-silenced, $p = 0.0009$; *Gr43a/Ir60b*-protected vs *Ir25a*-silenced, $p < 0.0001$; *Gr43a/Ir67c*-protected vs *Ir25a*-silenced, $p = 0.0007$; D-glucose peak duration: Kruskal–Wallis statistics = 43.13, *Gr43a*-protected vs *Ir25a*-silenced, $p < 0.0001$; *Gr43a/Ir60b*-protected vs *Ir25a*-silenced, $p < 0.0001$; *Gr43a/Ir67c*-protected vs *Ir25a*-silenced, $p < 0.0001$) and L-glucose (Fig. 7*F*; L-glucose peak intensity: Kruskal–Wallis statistics = 28.74, *Gr43a*-protected vs *Ir25a*-silenced, $p = 0.0006$; *Gr43a/Ir60b*-protected vs *Ir25a*-silenced, $p < 0.0001$; *Gr43a/Ir67c*-protected vs *Ir25a*-silenced, $p < 0.0001$; L-glucose peak duration: Kruskal–Wallis statistics = 25.6, *Gr43a*-protected vs *Ir25a*-silenced, $p = 0.0001$; *Gr43a/Ir60b*-protected vs *Ir25a*-silenced, $p = 0.0001$; *Gr43a/Ir67c*-protected vs *Ir25a*-silenced, $p < 0.0001$), supporting their role in controlling feeding responses to both sugars. Interestingly, when both *Gr43a* and *Ir67c* GRNs were protected, there was a significant increase in the duration of the first feeding event for D-glucose (D-glucose peak intensity: Kruskal–Wallis statistics = 1.295, *Gr43a*-protected vs *Gr43a/Ir60b*-protected, $p = 0.2818$; *Gr43a*-protected vs *Gr43a/Ir67c*-protected, $p = 0.8939$; D-glucose peak duration: Kruskal–Wallis statistics = 4.012, *Gr43a*-protected vs *Gr43a/Ir60b*-protected, $p = 0.2229$; *Gr43a*-protected vs *Gr43a/Ir67c*-protected, $p = 0.0499$) but not L-glucose (L-glucose peak intensity: Kruskal–Wallis statistics = 2.634, *Gr43a*-protected vs *Gr43a/Ir60b*-protected, $p = 0.1068$; *Gr43a*-protected vs *Gr43a/Ir67c*-protected, $p = 0.3481$; L-glucose peak duration: Kruskal–Wallis statistics = 0.5774, *Gr43a*-protected vs *Gr43a/Ir60b*-protected, $p = 0.9341$; *Gr43a*-protected vs *Gr43a/Ir67c*-protected, $p = 0.4839$) as compared with flies in which only *Gr43a* GRNs were protected (Fig. 7*E–F*). Therefore, *Ir67c* GRNs may differentially modulate *Gr43a* GRN-driven feeding responses to different sugars.

Inducible activation of pharyngeal *Gr43a* GRNs indicates functional subdivision by location

Anatomical and functional differences between sweet taste neurons in the legs have been reported previously in that sweet GRNs projecting to the ventral nerve cord control locomotion, whereas those projecting to the subesophageal zone control proboscis extension (Thoma et al., 2016). We therefore wondered whether functional differences exist between internal and external taste circuits. To address this, we examined behavioral outcomes of inducible activation of different subsets of sweet GRNs. We expressed red-shifted channelrhodopsin (*UAS-CsChrimson*; Klapoetke et al., 2014) in selected GRNs, induced activation by exposing flies to 626 nm red LEDs (Fig. 8*A*), and scored the number of proboscis extensions (Fig. 8*B–C*). Similar to previous reports (Keene and Masek, 2012; Dawydow et al., 2014; Inagaki et al., 2014), activation of all *Gr64e* GRNs in otherwise wild-type flies, which include both external and internal sweet GRNs, caused proboscis extensions (Fig. 8*D*; Movie 1; $F_{(4,380)} = 38.6$; *Gr64e-GAL4^{II}>CsChrimson* dark 1, $p = 0.998$ vs *UAS* control, $p = 0.998$ vs *GAL4* control; *Gr64e-GAL4^{III}>CsChrimson* dark 1, $p = 0.886$ vs *UAS* control, $p = 0.886$ vs *GAL4* control; *Gr64e-GAL4^{II}>CsChrimson* light 1, $p < 0.0001$ vs *UAS* control, $p < 0.0001$ vs *GAL4* control; *Gr64e-GAL4^{III}>CsChrimson* light 1, $p < 0.0001$ vs *UAS* control, $p < 0.0001$ vs *GAL4* control; *Gr64e-GAL4^{II}>CsChrimson* dark 2, $p = 0.998$ vs *UAS* control, $p = 0.5328$ vs *GAL4* control; *Gr64e-GAL4^{III}>CsChrimson* dark 2, $p > 0.9999$ vs *UAS* control, $p = 0.7296$ vs *GAL4* control; *Gr64e-GAL4^{II}>CsChrimson* light 2, $p < 0.0001$ vs *UAS* control, $p < 0.0001$ vs *GAL4* control; *Gr64e-GAL4^{III}>CsChrimson* light 2, $p < 0.0001$ vs *UAS* control, $p < 0.0001$ vs *GAL4* control; two-way ANOVA; Tukey's multiple comparisons test). Activation of *Gr64e* GRNs in *Poxn* mutants, which only include internal pharyngeal sweet GRNs, did not induce proboscis extensions (Fig. 8*E*; Movie 2; $F_{(4,380)} = 3.764$; *Poxn, Gr64e-GAL4^{II}>CsChrimson* dark 1, $p = 0.8592$ vs *UAS* control, $p = 0.9877$ vs *GAL4* control; *Poxn, Gr64e-GAL4^{III}>CsChrimson* dark 1, $p = 0.8538$ vs *UAS* control, $p > 0.9999$ vs *GAL4* control; *Poxn, Gr64e-GAL4^{II}>CsChrimson* light 1, $p = 0.9877$ vs *UAS* control, $p = 0.5716$ vs *GAL4* control;

←

dashed lines indicate median and the first and third quartiles, respectively. Asterisks (black) indicate significant difference from taste-blind (*Poxn; Ir25a*-silenced) flies by Kruskal–Wallis test followed by uncorrected Dunn's test; ***$p < 0.001$, ****$p < 0.0001$. Asterisks (red) indicate significant difference from *Poxn; Gr43a*-protected flies by Kruskal–Wallis test followed by uncorrected Dunn's test; *$p < 0.05$, ****$p < 0.0001$. ns, Not significant. Genotypes, left to right, *Poxn$^{\Delta M22\text{-}B5}$*, *Ir25a-GAL4/Poxn^{70}*; *UAS-Kir2.1/UAS-Kir2.1* and *Poxn$^{\Delta M22\text{-}B5}$*, *Ir25a-GAL4/Poxn^{70}*, *lexAop2-GAL80*; *Gr43a-LexA/UAS-Kir2.1* and *Poxn$^{\Delta M22\text{-}B5}$*, *Ir25a-GAL4/Poxn^{70}*, *lexAop2-GAL80*; *Gr43a-LexA*, *Ir60b-LexA/UAS-Kir2.1 and Poxn$^{\Delta M22\text{-}B5}$*, *Ir25a-GAL4/Poxn^{70}*, *lexAop2-GAL80*; *Gr43a-LexA*, *Ir67c-LexA/UAS-Kir2.1*.

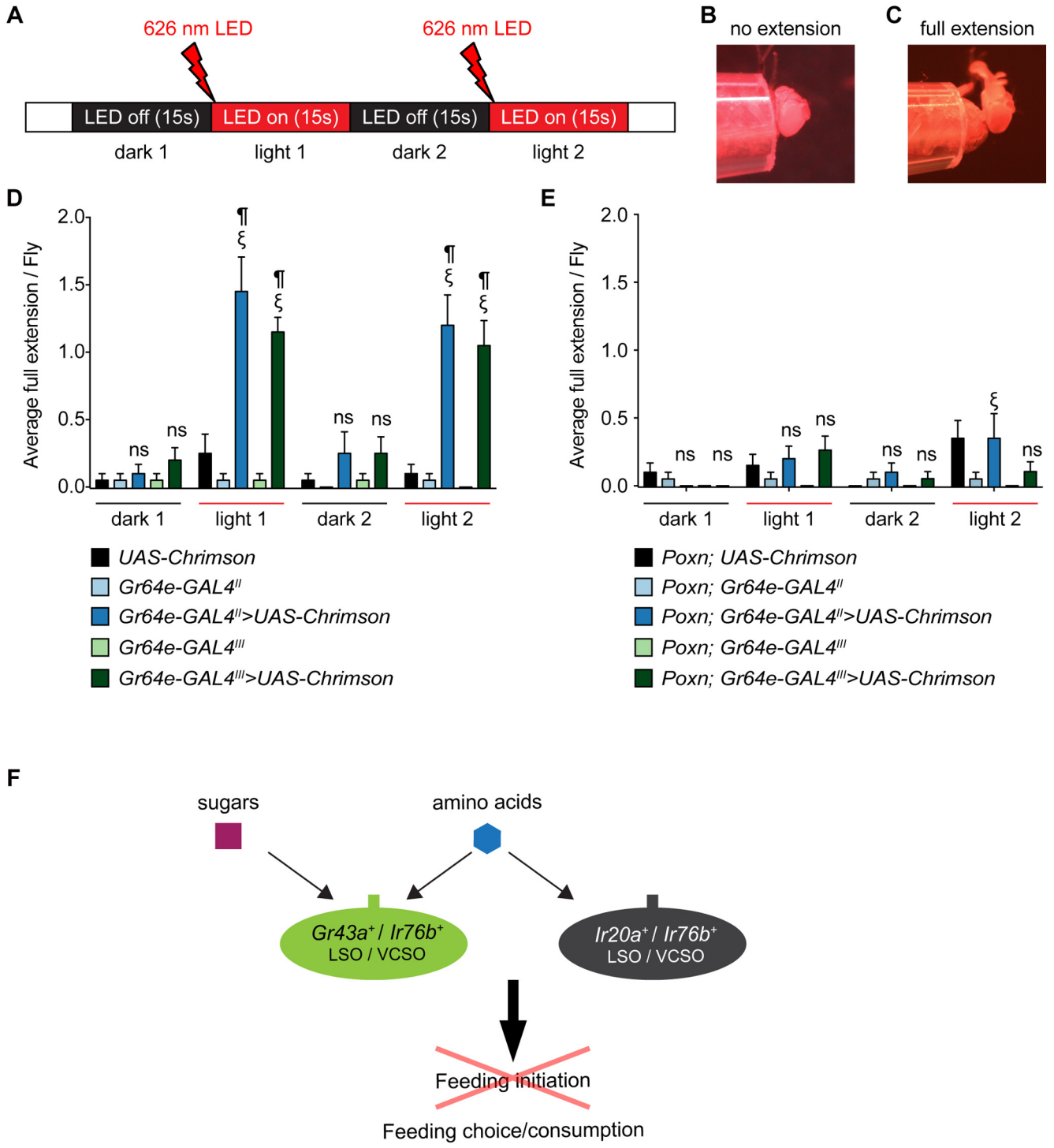

Figure 8. Inducible activation of pharyngeal *Gr43a* neurons does not induce proboscis extensions. ***A***, Schematic diagram of experimental procedure to test number of proboscis extensions in 15 s period before and during two consecutive sections of red light exposure from 626 nm LEDs. ***B***, ***C***, Examples of negative (***B***) and positive (***C***) full proboscis extension responses. ***D***, ***E***, Mean full proboscis extensions during red light exposure calculated for flies with indicated transgenes in a wild-type (***D***) or *Poxn* mutant background (***E***); $n = 19–21$. Error bars indicate SEM; ¶ indicates significant difference from the corresponding *UAS* control; ξ indicates significant difference from the corresponding *GAL4* control; $p < 0.05$, two-way ANOVA with *post hoc* Tukey test. ns, Not significant. Genotypes, left to right, (***D***) $^{+/+}$; *UAS-CsChrimson/+* and *Gr64e-GAL4/Sp*; *Dr or TM3/+* and *Gr64e-GAL4/Sp*; *UAS-CsChrimson/+* and *+/Sp*; *Gr64e-GAL4/+* and *+/Sp*; *Gr64e-GAL4/UAS-CsChrimson* (***E***) $Poxn^{\Delta M22\text{-}B5}/Poxn^{70}$; *UAS-CsChrimson/+* and $Poxn^{\Delta M22\text{-}B5}$, *Gr64e-GAL4/*$Poxn^{70}$ and $Poxn^{\Delta M22\text{-}B5}$, *Gr64e-GAL4/*$Poxn^{70}$; *UAS-CsChrimson/+* and $Poxn^{\Delta M22\text{-}B5}/Poxn^{70}$; *Gr64e-GAL4/+* and $Poxn^{\Delta M22\text{-}B5}/Poxn^{70}$; *Gr64e-GAL4/UAS-CsChrimson*. (***F***), A schematic summary of pharyngeal sugar and amino acid detection in driving food preference and consumption.

Poxn, Gr64e-GAL4^{III}*>CsChrimson* light 1, $p = 0.5599$ vs *UAS* control, $p = 0.0714$ vs *GAL4* control; *Poxn, Gr64e-GAL4*^{II}*>CsChrimson* dark 2, $p = 0.8592$ vs *UAS* control, $p = 0.9877$ vs *GAL4* control; *Poxn, Gr64e-GAL4*^{III}*>CsChrimson* dark 2, $p > 0.9999$ vs *UAS* control, $p = 0.9852$ vs *GAL4* control; *Poxn, Gr64e-GAL4*^{II}*>CsChrimson* light 2, $p > 0.9999$ vs *UAS* control, $p = 0.0258$ vs *GAL4* control; *Poxn, Gr64e-GAL4*^{III}*>CsChrimson* light 2, $p = 0.1189$ vs *UAS* control,

Movie 1. Optogenetic activation of *Gr64e* GRNs in wild-type flies. [View online]

Movie 2. Optogenetic activation of *Gr64e* GRNs in *Poxn* mutant flies. [View online]

$p = 0.8356$ vs *GAL4* control; two-way ANOVA; Tukey's multiple comparisons test), suggesting functional separation of sweet taste circuits based on their location of origin. These results are consistent with the idea that external sweet GRNs, but not pharyngeal sweet GRNs, trigger proboscis extension and initiation of feeding behavior.

Discussion

In this study, we found that appropriate feeding responses to appetitive tastants (sugars and amino acids) as well as aversive tastants (denatonium, tartaric acid, and high salt) were abolished in taste-blind flies in binary choice assays. These taste-blind flies provided an opportunity to directly test the extent to which taste input is required for appropriate food selection as well as to probe functional contributions of individual types of GRNs in controlling food choice and first feeding event parameters. Notably, functional protection of pharyngeal *Gr43a* GRNs in otherwise taste-blind flies restored intensity discrimination in choice assays, as well as the first feeding event intensity and duration, in response to sweet and amino acid tastants. Analysis of other pharyngeal GRNs' roles uncovered redundant functionality in food choice assays for amino acids.

Taste input is critical for behavioral decisions in short-term feeding assays

We found that *Poxn* flies lacking all external GRNs were nevertheless capable of evaluating food substrates and making selections, displaying sensitivity to most if not all tastant categories including sweet, bitter, salt, acid, and amino acids. Moreover, pharyngeal taste was essential for the observed taste sensitivity of *Poxn* mutants; silencing all pharyngeal GRNs via *Ir25a-GAL4* in *Poxn* flies rendered the flies unable to discriminate tastants in binary choice assays and to sustain feeding intensity and duration in FLIC assays. Although our FLIC data suggest that an absence of pharyngeal input (*Ir25a*-silenced *Poxn*) depresses feeding intensity and duration, there are limitations in explicitly correlating these features with behavior in real time. Previous studies found that high signal intensities in FLIC corresponded with high proportions of flies that fed in each experiment, but even in this case food intake was not measured (Ro et al., 2014). We also note that that the conductivity of experimental food may influence signal intensity. To address this, we set a minimum intensity threshold of 100 units over the baseline for feeding events, ensuring that such events would be identified relative to an electrical signal of each well and tastant solution combination. Notwithstanding all these caveats, qualitative comparisons of the FLIC features are useful to understand how flies use pharyngeal taste input to motivate consumption. Importantly, the role of pharyngeal *Gr43a* GRNs in detecting sugars and amino acids is supported by FLIC analysis, in which no dyes with possible tastant interactions are used.

Taste peg GRNs are unlikely to be involved in detection of sugars and amino acids

It has been shown that some taste pegs are present in the *Poxn* mutant background (LeDue et al., 2015), and both *Ir25a-GAL4* and *Gr43a-LexA* label taste peg GRNs that respond to carbonated water and fatty acids (Fischler et al., 2007; Tauber et al., 2017; Sánchez-Alcañiz et al., 2018). It remains possible, although unlikely, that taste pegs rather than pharyngeal GRNs mediate the observed taste-driven behaviors for the following reasons. First, *Gr43a-LexA* only labeled taste peg projections in older flies but not younger flies that we used in this study (Extended Data Fig. 1-1). Second, previous Ca^{2+} imaging data show little if any response to sugars, or amino acids (serine and threonine), in taste peg GRNs (Fischler et al., 2007; Sanchez-Alcaniz et al., 2018). Third, carbonated water, the strongest tastant activator of taste peg GRNs, does not elicit consumption in feeding assays and only shows weak positional preference (Fischler et al., 2007; Sanchez-Alcaniz et al., 2018). Thus, the most parsimonious interpretation of all evidence is that pharyngeal *Gr43a* GRNs play a major role in mediating the observed taste-driven behaviors, whereas taste pegs have little if any behavioral contribution in this context.

Differential behavioral sensitivity to D-glucose and L-glucose in peripheral GRNs

Our results suggest that taste input is important for flies to choose D-glucose over L-glucose in short-term assays. The underlying sensory basis for this is still unclear as no differences have been found in physiological and/or behavioral sensitivity to D-glucose and L-glucose using recordings or proboscis extension assays (Fujita and Tanimura, 2011). Our findings suggest that pharyngeal *Gr43a* GRNs may represent one of the neural circuits that facilitate discrimination between the two sugars. Not only can *Gr43a*-protected *Poxn* flies select D-glucose over L-glucose in choice assays but they also exhibit differences in feeding features evoked by the two sugars. Such differential responses to D-sugars or L-sugars might not be a unique feature for pharyngeal GRNs because wild-type flies but not *UAS-Kir2.1 Poxn* control flies exhibited a preference for D-glucose over L-glucose (Fig. 6*C*), raising the possibility that some external sugar-sensing GRNs may possess similar qualities. Given that the previous study only surveyed L-type labellar hairs (Fujita and Tanimura,

2011), it is possible that other types of labellar or tarsal hairs have a higher sensitivity to D-glucose over L-glucose. In another example, differential sensory responses to D-arabinose and L-arabinose have been reported in the *Gr43a* GRNs in the tarsi and the LSO (McGinnis et al., 2016), supporting the ability of peripheral GRNs to distinguish structurally similar enantiomers of sugars.

Multimodal integration of tastant information in sensory neurons

The prevailing model of taste coding is that chemicals are separated into taste categories by their ability to activate defined, nonoverlapping subpopulations of taste neurons (Accolla et al., 2007; Chen et al., 2011; Barretto et al., 2015; Harris et al., 2015). Recent observations are beginning to build a more nuanced view of this idea (Chen and Dahanukar, 2020). For example, sweet and fatty acid tastes overlap in external GRNs (Ahn et al., 2017; Tauber et al., 2017), as do bitter and acid tastes (Charlu et al., 2013). In the context of a *Poxn* fly with a minimal taste system of 24 GRNs, genetic dissection analyses reveal that both appetitive and deterrent classes of GRNs sense chemicals belonging to more than one classically described taste category. In agreement with this idea, pharyngeal *Gr43a* GRNs are sufficient for promoting consumption of both sweet and amino acid tastants. In addition, our previous finding that the sugar response of pharyngeal *Gr43a* GRNs can be inhibited by the presence of bitter compounds, high concentrations of salt, or acid (Chen et al., 2019), suggests that pharyngeal *Gr43a* GRNs act as a hub to integrate information across many tastant categories. How do pharyngeal *Gr43a* GRNs respond to such a diversity of tastants? It is likely that different types of receptors are involved. Although sugar responses depend on Gr receptors, the amino acid response in *Gr43a* GRNs may depend on Ir76b, a broadly expressed ionotropic receptor that is required for amino acid response in external GRNs (Ganguly et al., 2017). It will be interesting to determine the molecular basis for recognition of other tastants in pharyngeal *Gr43a* GRNs. Alternatively, it is also possible that pharyngeal *Gr43a* GRNs consist of heterogenous subpopulations that respond to sugars and amino acids differentially. Future genetic dissection among these pharyngeal *Gr43a* GRNs would provide further tools to test this hypothesis.

Overall, an idea that emerges from our studies is that pharyngeal GRNs may encode valence rather than tastant category. How generalizable are these findings to the taste system as a whole? It is possible that the pharynx may be unique by virtue of its distinctive groupings of neurons and chemosensory receptor coexpression patterns. However, some larval GRNs have been found to detect multiple tastant categories (van Giesen et al., 2016), and many external GRNs also coexpress members of the Gr, Ir, and ppk families (Thistle et al., 2012; Ahn et al., 2017; Chen and Amrein, 2017) and may have broader functions than conceived so far. Multimodal sensing properties also invite questions of whether each GRN class can independently modulate sensitivities to different tastant categories in ways that reflect the nutritional needs of an animal. It will be interesting to determine how the response of *Gr43a* GRNs to sugars and amino acids relates to the postmating increase in feeding preference for amino acids relative to sugars in females (Ribeiro and Dickson, 2010; Ganguly et al., 2017).

Functional redundancies between different classes of taste neurons

Behavioral analyses of flies in which only single classes of pharyngeal GRNs are active, combined with analysis of flies in which single classes of pharyngeal GRNs are silenced, uncover an unforeseen degree of functional redundancy in the pharynx. For example, we find that although *Gr43a* GRNs are sufficient to promote amino acid feeding, amino acid preference is abolished only upon silencing both *Ir20a* and *Gr43a* GRNs (Fig. 5*D*). These results are consistent with our previous findings of a role for the Ir20a receptor in amino acid taste (Ganguly et al., 2017). Because *Ir20a-GAL4* expression does not overlap with pharyngeal *Gr43a* GRNs, there may be at least two distinct pathways for sensing amino acids, one (*Ir20a*-independent) in pharyngeal *Gr43a* GRNs and another (*Ir20a*-dependent) in the *Ir20a*-expressing neurons. Interestingly, silencing of *ppk28-GAL4* labeled GRNs, which include all *Ir20a*-labeled GRNs with the exception of the V3 neuron, did not significantly disrupt amino acid response. Thus, the V3 neuron is a candidate for an *Ir20a* GRN that acts in parallel with pharyngeal *Gr43a* GRNs to sense amino acids. It will be interesting to determine whether pharyngeal *Gr43a* and *Ir20a* GRNs can detect different amino acids.

References

Accolla R, Bathellier B, Petersen CC, Carleton A (2007) Differential spatial representation of taste modalities in the rat gustatory cortex. J Neurosci 27:1396–1404.

Ahn JE, Chen Y, Amrein H (2017) Molecular basis of fatty acid taste in *Drosophila*. Elife 6:e30115.

Awasaki T, Kimura K (1997) pox-neuro is required for development of chemosensory bristles in *Drosophila*. J Neurobiol 32:707–721.

Baines RA, Uhler JP, Thompson A, Sweeney ST, Bate M (2001) Altered electrical properties in *Drosophila* neurons developing without synaptic transmission. J Neurosci 21:1523–1531.

Barretto RP, Gillis-Smith S, Chandrashekar J, Yarmolinsky DA, Schnitzer MJ, Ryba NJ, Zuker CS (2015) The neural representation of taste quality at the periphery. Nature 517:373–376.

Boll W, Noll M (2002) The *Drosophila* Pox neuro gene: control of male courtship behavior and fertility as revealed by a complete dissection of all enhancers. Development 129:5667–5681.

Cameron P, Hiroi M, Ngai J, Scott K (2010) The molecular basis for water taste in *Drosophila*. Nature 465:91–95.

Charlu S, Wisotsky Z, Medina A, Dahanukar A (2013) Acid sensing by sweet and bitter taste neurons in *Drosophila melanogaster*. Nat Commun 4:2042.

Chen X, Gabitto M, Peng Y, Ryba NJ, Zuker CS (2011) A gustotopic map of taste qualities in the mammalian brain. Science 333:1262–1266.

Chen Y, Amrein H (2017) Ionotropic receptors mediate *Drosophila* oviposition preference through sour gustatory receptor neurons. Curr Biol 27:2741–2750.e4.

Chen YD, Dahanukar A (2017) Molecular and cellular organization of taste neurons in adult *Drosophila* pharynx. Cell Rep 21:2978–2991.

Chen YD, Dahanukar A (2020) Recent advances in the genetic basis of taste detection in *Drosophila*. Cell Mol Life Sci 77:1087–1101.

Chen YD, Park SJ, Ja WW, Dahanukar A (2018) Using *Pox-neuro* (*Poxn*) mutants in *Drosophila* gustation research: a double-edged sword. Front Cell Neurosci 12:382.

Chen YD, Park SJ, Joseph RM, Ja WW, Dahanukar AA (2019) Combinatorial pharyngeal taste coding for feeding avoidance in adult *Drosophila*. Cell Rep 29:961–973.e4.

Dahanukar A, Lei YT, Kwon JY, Carlson JR (2007) Two Gr genes underlie sugar reception in *Drosophila*. Neuron 56:503–516.

Dawydow A, Gueta R, Ljaschenko D, Ullrich S, Hermann M, Ehmann N, Gao S, Fiala A, Langenhan T, Nagel G, Kittel RJ (2014) Channelrhodopsin-2-XXL, a powerful optogenetic tool for low-light applications. Proc Natl Acad Sci U S A 111:13972–13977.

Devineni AV, Sun B, Zhukovskaya A, Axel R (2019) Acetic acid activates distinct taste pathways in *Drosophila* to elicit opposing, state-dependent feeding responses. Elife 8:

Dus M, Min S, Keene AC, Lee GY, Suh GS (2011) Taste-independent detection of the caloric content of sugar in *Drosophila*. Proc Natl Acad Sci U S A 108:11644–11649.

Dus M, Lai JS, Gunapala KM, Min S, Tayler TD, Hergarden AC, Geraud E, Joseph CM, Suh GS (2015) Nutrient sensor in the brain directs the action of the brain-gut axis in *Drosophila*. Neuron 87:139–151.

Dweck HKM, Carlson JR (2020) Molecular logic and evolution of bitter taste in *Drosophila*. Curr Biol 30:17–30.e3.

Fan P, Manoli DS, Ahmed OM, Chen Y, Agarwal N, Kwong S, Cai AG, Neitz J, Renslo A, Baker BS, Shah NM (2013) Genetic and neural mechanisms that inhibit *Drosophila* from mating with other species. Cell 154:89–102.

Fischler W, Kong P, Marella S, Scott K (2007) The detection of carbonation by the *Drosophila* gustatory system. Nature 448:1054–1057.

Freeman EG, Dahanukar A (2015) Molecular neurobiology of *Drosophila* taste. Curr Opin Neurobiol 34:140–148.

Fujii S, Yavuz A, Slone J, Jagge C, Song X, Amrein H (2015) *Drosophila* sugar receptors in sweet taste perception, olfaction, and internal nutrient sensing. Curr Biol 25:621–627.

Fujita M, Tanimura T (2011) *Drosophila* evaluates and learns the nutritional value of sugars. Curr Biol 21:751–755.

Ganguly A, Pang L, Duong VK, Lee A, Schoniger H, Varady E, Dahanukar A (2017) A molecular and cellular context-dependent role for Ir76b in detection of amino acid taste. Cell Rep 18:737–750.

Harris DT, Kallman BR, Mullaney BC, Scott K (2015) Representations of taste modality in the *Drosophila* brain. Neuron 86:1449–1460.

Inagaki HK, Jung Y, Hoopfer ED, Wong AM, Mishra N, Lin JY, Tsien RY, Anderson DJ (2014) Optogenetic control of *Drosophila* using a red-shifted channelrhodopsin reveals experience-dependent influences on courtship. Nat Methods 11:325–332.

Jaeger AH, Stanley M, Weiss ZF, Musso PY, Chan RC, Zhang H, Feldman-Kiss D, Gordon MD (2018) A complex peripheral code for salt taste in *Drosophila*. Elife 7:e37167.

Jiao Y, Moon SJ, Wang X, Ren Q, Montell C (2008) Gr64f is required in combination with other gustatory receptors for sugar detection in *Drosophila*. Curr Biol 18:1797–1801.

Joseph RM, Sun JS, Tam E, Carlson JR (2017) A receptor and neuron that activate a circuit limiting sucrose consumption. Elife 6:e24992.

Keene AC, Masek P (2012) Optogenetic induction of aversive taste memory. Neuroscience 222:173–180.

Klapoetke NC, Murata Y, Kim SS, Pulver SR, Birdsey-Benson A, Cho YK, Morimoto TK, Chuong AS, Carpenter EJ, Tian Z, Wang J, Xie Y, Yan Z, Zhang Y, Chow BY, Surek B, Melkonian M, Jayaraman V, Constantine-Paton M, Wong GK-S, et al. (2014) Independent optical excitation of distinct neural populations. Nat Methods 11:338–346.

Koh TW, He Z, Gorur-Shandilya S, Menuz K, Larter NK, Stewart S, Carlson JR (2014) The *Drosophila* IR20a clade of ionotropic receptors are candidate taste and pheromone receptors. Neuron 83:850–865.

LeDue EE, Chen YC, Jung AY, Dahanukar A, Gordon MD (2015) Pharyngeal sense organs drive robust sugar consumption in Drosophila. Nat Commun 6:6667.

Liman ER, Zhang YV, Montell C (2014) Peripheral coding of taste. Neuron 81:984–1000.

Ling F, Dahanukar A, Weiss LA, Kwon JY, Carlson JR (2014) The molecular and cellular basis of taste coding in the legs of *Drosophila*. J Neurosci 34:7148–7164.

McGinnis JP, Jiang H, Agha MA, Sanchez CP, Lange J, Yu Z, Marion-Poll F, Si K (2016) Immediate perception of a reward is distinct from the reward's long-term salience. Elife 5:e22283.

Miyamoto T, Amrein H (2014) Diverse roles for the *Drosophila* fructose sensor Gr43a. Fly (Austin)) 8:19–25.

Miyamoto T, Slone J, Song X, Amrein H (2012) A fructose receptor functions as a nutrient sensor in the *Drosophila* brain. Cell 151:1113–1125.

Nottebohm E, Dambly-Chaudière C, Ghysen A (1992) Connectivity of chemosensory neurons is controlled by the gene poxn in *Drosophila*. Nature 359:829–832.

Park JH, Kwon JY (2011) Heterogeneous expression of *Drosophila* gustatory receptors in enteroendocrine cells. PLoS One 6:e29022.

Ribeiro C, Dickson BJ (2010) Sex peptide receptor and neuronal TOR/S6K signaling modulate nutrient balancing in *Drosophila*. Curr Biol 20:1000–1005.

Ro J, Harvanek ZM, Pletcher SD (2014) FLIC: high-throughput, continuous analysis of feeding behaviors in *Drosophila*. PLoS One 9:e101107.

Sánchez-Alcañiz JA, Silbering AF, Croset V, Zappia G, Sivasubramaniam AK, Abuin L, Sahai SY, Münch D, Steck K, Auer TO, Cruchet S, Neagu-Maier GL, Sprecher SG, Ribeiro C, Yapici N, Benton R (2018) An expression atlas of variant ionotropic glutamate receptors identifies a molecular basis of carbonation sensing. Nat Commun 9:4252.

Slone J, Daniels J, Amrein H (2007) Sugar receptors in *Drosophila*. Curr Biol 17:1809–1816.

Stafford JW, Lynd KM, Jung AY, Gordon MD (2012) Integration of taste and calorie sensing in *Drosophila*. J Neurosci 32:14767–14774.

Tauber JM, Brown EB, Li Y, Yurgel ME, Masek P, Keene AC (2017) A subset of sweet-sensing neurons identified by IR56d are necessary and sufficient for fatty acid taste. PLoS Genet 13:e1007059.

Thistle R, Cameron P, Ghorayshi A, Dennison L, Scott K (2012) Contact chemoreceptors mediate male-male repulsion and male-female attraction during *Drosophila* courtship. Cell 149:1140–1151.

Thoma V, Knapek S, Arai S, Hartl M, Kohsaka H, Sirigrivatanawong P, Abe A, Hashimoto K, Tanimoto H (2016) Functional dissociation in sweet taste receptor neurons between and within taste organs of *Drosophila*. Nat Commun 7:10678.

van Giesen L, Hernandez-Nunez L, Delasoie-Baranek S, Colombo M, Renaud P, Bruggmann R, Benton R, Samuel ADT, Sprecher SG (2016) Multimodal stimulus coding by a gustatory sensory neuron in *Drosophila* larvae. Nat Commun 7:10687.

Weiss LA, Dahanukar A, Kwon JY, Banerjee D, Carlson JR (2011) The molecular and cellular basis of bitter taste in *Drosophila*. Neuron 69:258–272.